Journal of Environmental Management 359 (May 2024) 121017

Preprint article

Experimental assessment of pollutant emissions from residential fuel cells and comparative benchmark analysis

Paulus, N. [a,b]*, Lemort, V. [b]

[a] *Department of Electromechanics, Industrial Engineering Higher Education Institution of the Province of Liège (HEPL), Liège, 4000, Belgium*

[b] *Department of Aerospace and Mechanics, University of Liège, Liège, 4000, Belgium*

E-mail address: nicolas.paulus@hepl.be (N. Paulus).

https://doi.org/10.1016/j.jenvman.2024.121017

Received 20 December 2023; Received in revised form 16 April 2024; Accepted 23 April 2024
Available online 7 May 2024

Abstract:

Energy transition currently brings focus on fuel cell micro-combined heat and power (mCHP) systems for residential uses. The two main technologies already commercialized are the Proton Exchange Membrane Fuel Cells (PEMFCs) and Solid Oxide Fuel Cells (SOFCs). The pollutant emissions of one system of each technology have been tested with a portable probe both in laboratory and field-test configurations. In this paper, the nitrogen oxides (NO_x), sulphur dioxide (SO_2), and carbon monoxide (CO) emission levels are compared to other combustion technologies such as a recent Euro 6 diesel automotive vehicle, a classical gas condensing boiler, and a gas absorption heat pump. At last, a method of converting the concentration of pollutants (in ppm) measured by the sensors into pollutant intensity per unit of energy (in mg/kWh) is documented and reported. This allows for comparing the pollutant emissions levels with relevant literature, especially other studies conducted with other measuring sensors.

Both tested residential fuel cell technologies fed by natural gas can be considered clean regarding SO_2 and NO_x emissions. The CO emissions can be considered quite low for the tested SOFC and even nil for the tested PEMFC. The biggest issue of natural gas fuel cell technologies still lies in the carbon dioxide (CO_2) emissions associated with the fossil fuel they consume. The gas absorption heat pump however shows worse NO_x and CO levels than the classical gas condensing boiler.

At last, this study illustrates that the high level of hybridization between a fuel cell and a gas boiler may be responsible for unexpected ON/OFF cycling behaviours and therefore prevent both sub-systems from operating as optimally and reliably as they would have as standalone units.

Keywords:

SO_2, Fuel cell, emission factor, NO_x, pollutant emissions, CO.

1. Introduction

In its latest Sixth Assessment Report in April 2022, the Intergovernmental Panel on Climate Change has reported a maximum carbon budget of 890 $GtCO_2$ that humanity can emit from January 1st 2020 in order for global warming to likely remain under the +2 °C widely acknowledged limit compared to preindustrial temperature levels (Paulus, 2023). Even at residential scales, this much-needed GreenHouse Gases (GHG) mitigation brings focus to cleaner power sources and combined heat and power (CHP) systems, such as fuel cells (Dávila et al., 2022a). The two primary technologies that have already been commercialized are the Proton Exchange Membrane Fuel Cells (PEMFCs) and the Solid Oxide Fuel Cells (SOFCs), which are later on compared in Table 1. GHG emissions (in terms of CO_2 or CO_{2eq}) of such systems have already been addressed in previous studies (Paulus et al., 2022a;

*Corresponding author. Quai Gloesener No. 6, 4000 Liège, Belgium
Email address: nicolas.paulus@hepl.be

Paulus and Lemort, 2022a) but another key element in assessing the environmental impacts of those technologies lies in the other common air pollutants: the emissions of nitrogen oxides (NO_x), sulphur dioxide (SO_2), and carbon monoxide (CO).

The novelty of this study lies within the evaluation of SO_2, NO_x, and CO emissions of fuel cell technologies commercialized for residential applications in both laboratory and field-test configurations (in real dwellings in Belgium). This has been performed on several machines of different ages, for one PEMFC-based and one SOFC-based micro-combined heat and power (mCHP) technology, thanks to a combustion analyser portable meter. This study compares the emission levels of those pollutants, measured for the studied fuel cell systems, with other combustion technologies, such as a recent Euro 6 diesel automotive vehicle and classical gas condensing boilers. To facilitate comparison with relevant literature, a method to convert sensor-detected pollutant concentrations (measured in ppm) into pollutant intensity per unit of energy (in g/kWh) has been documented and reported in this study. This represents another unprecedented contribution to academic literature, as far as the authors are aware. This approach indeed enables the assessment of pollutant emissions levels across different studies, including those conducted using alternative measuring sensors.

It is noteworthy that the initial study upon which this research builds was presented at a conference (Paulus and Lemort, 2023a) and subsequently selected for publication in this journal. However, this paper still delivers new results and novel analyses distinct from the earlier work.

2. Background

2.1 SOFC and PEMFC current technologies

In residential systems currently commercialized, SOFC technology is characterized by its oxygen ion-conducting electrolyte, usually a (solid) ceramic that includes oxides (Nicolas Paulus, 2024a, 2024b). The charge carrier therefore consists of oxygen ions, leading to the common 'O-SOFC' more explicit acronym (Nicolas Paulus, 2024a) and its working principle is depicted in Figure 1(a), reproduced and adapted from reference (Guney and Tepe, 2017). Oppositely, currently commercialized PEMFC systems only consist of LT-PEMFCs (Low-Temperature Proton Exchange Membrane Fuel Cells), characterized by a (solid) polymer electrolyte that is permeable to protons, i.e. hydrogen cations (Nicolas Paulus, 2024a, 2024b). Its working principle is presented in Figure 1(b), reproduced and adapted from reference (Alshorman, 2016).

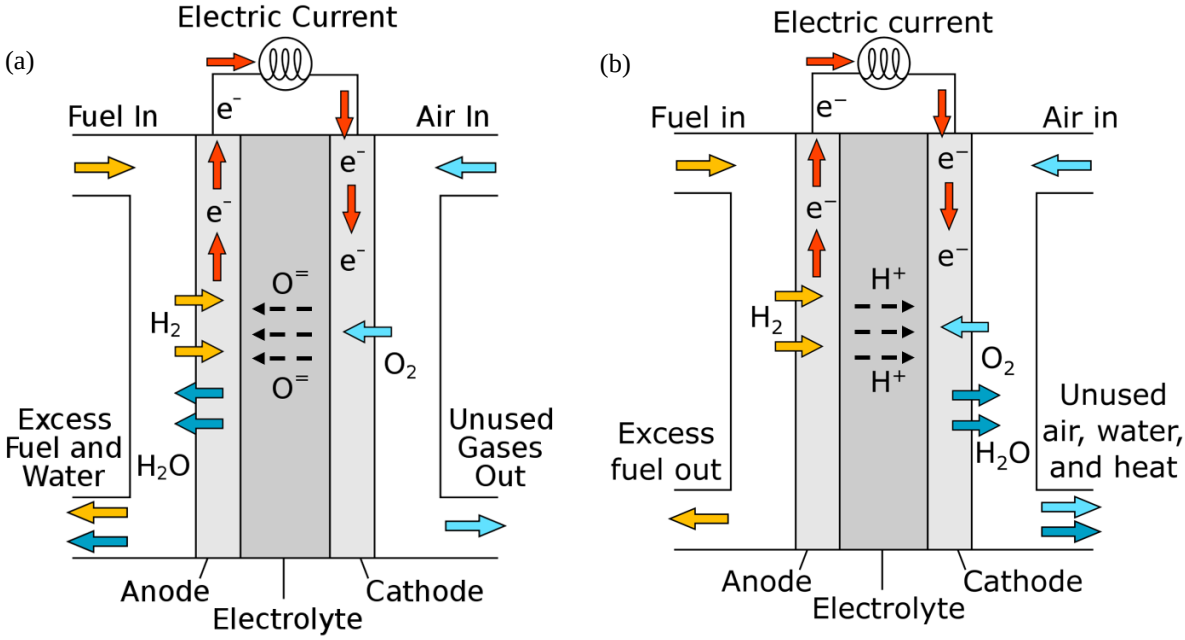

Figure 1. Working principle of the two existing residential fuel cell technologies. It is noteworthy that the respective charge carriers have opposite charges in both technologies and therefore flow through the respective electrolytes in opposite directions. (a) O-SOFC. Reproduced and adapted from reference (Guney and Tepe, 2017); (b) PEMFC (valid for Low-Temperature and High-Temperature PEMFCs). Reproduced and adapted from reference (Alshorman, 2016).

A detailed comparison of these two technologies has been provided in Table 1. Besides their distinctive charge carriers and electrolytes, Solid Oxide Fuel Cells (SOFCs) operate at a markedly higher temperature, approximately

1000°C, whereas Proton Exchange Membrane Fuel Cells (PEMFCs) function at temperatures below 100°C. This substantially higher stack operating temperature of SOFCs involves drawbacks, such as low startup time, higher thermal stresses, higher costs, *etc*, but also leads to significantly higher fuel flexibility, tolerance to contaminants, and electrical efficiency (when operated on hydrocarbons).

Table 1.
Comparison between PEMFCs and SOFCs. Reproduced and adapted from references (Nicolas Paulus, 2024a; Sharaf and Orhan, 2014).

Fuel cell type & Charge carrier	Typical electrolyte	Major contaminants	Stack operating temperature (°C)	Specific advantages	Specific disadvantages	LHV Electrical efficiency (%)
PEMFC & H+	Solid Nafion®, a polymer	Carbon monoxide (CO) [a] Hydrogen sulfide (H_2S) [a]	60–80 Only low-temperature PEMFCs are currently commercialized (Element Energy, 2021)	Highly modular for most applications High power density Compact structure Rapid startup due to low-temperature operation Excellent dynamic response	Complex water and thermal management [a] Low-grade heat High sensitivity to contaminants [d] Expensive catalyst Expensive Nafion® membrane (Park and Hong, 2016) Low fuel flexibility	40-60 (with H_2) Currently limited to 38.5 with CH_4 as some fuel needs to be burned to provide heat to a methane reformer (Perna and Minutillo, 2020)
SOFC & O^{2-}	Solid yttria-stabilized zirconia, i.e. YSZ, a ceramic	Sulfides	800-1000	High electrical efficiencies High-grade heat High tolerance to contaminants Possibility of internal reforming Fuel flexibility Inexpensive catalyst Simpler water management - SOFC can work in a perfect drying state (Wen, 2002)	Slow startup Low power density Strict material requirements High thermal stresses Sealing issues Durability issues High manufacturing costs	55-65 (with H_2) Currently limited to 60%-65% with CH_4 (Bloom Energy, 2023; Element Energy, 2021), i.e. still high thanks to the SOFC fuel flexibility

[a] Contaminants, thermal, and water management of PEMFC stacks have been discussed more deeply in another work (Paulus et al., 2024).

2.2 Harmful effects of NO_x, SO_2, and CO

2.2.1 NO_x

Nitrogen oxides, i.e. NO_x, in the ambient air consist primarily of nitric oxide, i.e. NO, and the much more harmful nitrogen dioxide, i.e. NO_2 (Cheremisinoff, 2002), that NO readily turns into in the atmosphere in the presence of volatile organic compounds (Cheremisinoff, 2002), i.e. VOCs (Cheremisinoff and Young, 1977). NO_2 indeed irritates the lungs and promotes respiratory infections (Gupta, 2018). The two forms of gaseous nitrogen oxides are not only considered as pollutants of the lower atmosphere, but they also can have a significant impact on the upper atmosphere. Indeed, NO_2 has been reported to contribute to acid rain (Cheremisinoff, 2002), which subsequently, in addition to endangering vegetation, ecosystems and freshwater (Cheremisinoff, 2002) or increase human exposure to nitrate/nitrite consumption (Galloway et al., 2013), enhance the soil nitrous oxide (N_2O) emissions (Cao et al., 2021; Thomson et al., 2012). In fact, this strong GHG pollutant, with a global warming potential over 100 years that is evaluated about 300 times greater than CO_2 (Muret et al., 2019), is also responsible for most of the stratospheric ozone depletion (Portmann et al., 2012). It is worth mentioning that, through the subsequent formation of N_2O, the global warming potential over 100 years of NO_x is estimated between 7 and 10 (Lammel and Graßl, 1995).

In the lower atmosphere, in addition to being again a precursor of acid precipitation, it is also a precursor of fine particulate matter (Kuo et al., 2017), which can penetrate deep into vital systems, causing cardiovascular and respiratory diseases (Peng, 2008) as bad as lung cancers (Hamra et al., 2014), increasing morbidity and mortality (Brook et al., 2010). Nitrogen dioxide is also a precursor of tropospheric ozone (O_3) formation (Cheremisinoff, 2002). And O_3 is a poison even more harmful than NO_2 (Gupta, 2018). Indeed, it damages vegetation, irritates lung tissues, and can lead to smog, even more harmful to respiratory functions than ozone (Cheremisinoff, 2002). Smog is known to cause deaths as it can coarse many other pollutants of different toxicities, such as particulate matter (Mishra, 2017). Indeed, smog primarily consists of ozone and ‘secondary’ pollutants that are produced through photochemical reactions of directly emitted species, mainly consisting once again of VOCs (Sher, 1998),

in processes that are driven by sunlight and accelerated by warm temperatures (Sillman, 2003). The chemical composition of smog can vary according to mereological conditions, primarily temperature, humidity, and radiation (Raza et al., 2021). It also specifically varies according to the concentration of other pollutants (not only VOCs) and other atmospheric species (Raza et al., 2021). For example, the effect of smog is even aggravated when it contains fine particulate matter (Jiang et al., 2016). Smog can also contain and induce the health issues of the following species: lead (Grzywa-Celińska et al., 2020), peroxylacyl nitrates (PAN), aldehydes, CO, SO_2, NO_x (Raza et al., 2021) or their sulphate/nitrate derivatives (Zhou et al., 2015), etc.

2.2.2 SO_2

Similarly to NO_2, SO_2 is a major precursor of acid rains and fine particulate matter (Geddes and Murphy, 2012) and can thus be associated with their environmental and health issues. Another similarity is that it is an irritating gas that leads to respiratory illnesses (Cheremisinoff, 2002). It also has been reported that it can aggravate existing heart (and pulmonary) diseases (Hanrahan, 2012). Oppositely to NO_x, SO_2 has a negative contribution to global warming with a GWP100 estimated between -18 and -25 (Rypdal et al., 2009). This is because SO_2 is a precursor of sulphate or sulfuric acid aerosols (Gupta, 2018). It is noteworthy that decreasing the emissions of those negative forcing aerosol pollutants will unfortunately have the unwanted consequence of increasing net radiative forcing, which is commonly called as an 'unmasking' effect (N. Paulus, 2024).

While SO_2 is not a direct precursor of ozone, it has been reported that sulfur compounds initiated by SO_2 emissions can function similarly to VOCs in the ozone formation cycle, in a mechanism of re-oxidation of NO into NO_2, following the reaction of NO_2 with O_2 to form O_3 and NO (Graedel, 1976). At last, as stated, it can aggravate smog toxicity. This can occur either directly (Grzywa-Celińska et al., 2020), through its sulphate derivatives (Zhou et al., 2015), or through the fine particulate matter it can coarse into (Geddes and Murphy, 2012; Raza et al., 2021).

2.2.3 CO

CO is a well-known major air pollutant as it is also known as the 'silent killer' (invisible and odourless): at a concentration of 12000 ppm, it kills in two to three breaths as it blocks the ability of haemoglobin to transport oxygen to the cells of the body (Varma et al., 2015). However, at lower concentrations, it also has many impacts on human health: impaired vision, reduced brain function (Hanrahan, 2012), coma, seizures, heart and respiratory diseases, physical weakness (Gupta, 2018), tissue damage (Eichhorn et al., 2018). It is also considered as a minor ozone precursor in urban areas as it can play the role of VOCs in the ozone formation cycle (Chameides et al., 1992). At last, even though the lifetime of CO in the atmosphere is quite short, i.e. a few months (Rotmans and Den Elzen, 1992), its GWP100 is still estimated at 5 because of its interaction with methane (Rotmans and Den Elzen, 1992). Indeed, this is mainly because the main removal process of both CO and CH_4 includes the reaction with hydroxyl radicals (Johnson and Derwent, 1996). CO emissions reduce the hydroxyl radicals concentration for methane removal, which has a quite high GWP100 of about 28 (Paulus et al., 2022a), thus leading to a significant indirect impact of CO emissions on global warming.

2.3 SO_2 and NO_x emission factors of space heating appliances

SO_2 and NO_x emission factors of typical space heating appliances have respectively been reported in Table 2 and Table 3. The data required to feed such a comparative table relative to CO emission factors of typical space heating appliances (and Belgian grid electricity in Belgium) could not (yet) be computed with the literature review conducted through this study.

Table 2.
Combustion only and Life Cycle Assessment (LCA) SO_2 emission level reported from Energie+ (Energie+, 2007), which is a website developed by the University of Louvain-la-Neuve and the Energy Department of the Walloon Region, in Belgium. It is noteworthy that the electrical radiator emission factor has been established based on (and is therefore relevant for) the Belgian electrical mix.

Space-heating appliance	SO_2 (source from 2007: Fondation Rurale de Wallonie - combustion only) mg/kWh$_{th}$	SO_2 (source accessed in 2007: Gemis 4.5 - complete LCA cycle) mg/kWh$_{th}$
Oil-fired boiler	504	600
Gas condensing boiler	0[a]	111
Electrical radiators (Joule heating)	Unavailable	392[b]
Old log wood boiler	36	Unavailable
Modern log wood boiler	36	320
Wood chip boiler (wood chips)	36	Unavailable
Condensing wood boiler (pellets)	Unavailable	472

[a] Combustion-only SO_2 emissions from natural gas combustion are definitely low as most natural gas markets require less than 4 ppm of (all) sulfur-containing compounds in the gas (Speight, 2019). Indeed, decentralized desulfurization is implemented in natural gas processing (Xu et al., 2020). However, the SO_2 combustion-only emissions of gas condensing boilers are not completely nil as other studies have reported about 2 mg/khW$_{th}$ (Papadopoulo et al., 2011) or between 3.5 and 4 mg/khW$_{th}$ (Proszak-Miasik and Rabczak, 2018). This latter study considers a residential domestic hot water demand of 300 L a day at 45°C (Proszak-Miasik and Rabczak, 2018) and this has been considered to correspond to 12.3 kWh$_{th}$ a day (Fuentes et al., 2018).

[b] The power plant type has a strong influence on the SO_2 emissions. As a comparison, in 2012 in the US, coal-fired and Combined Cycle Gas Turbine (CCGT) power plants were reported to have average combustion-only SO_2 emission intensities respectively of about 1200 mg/kWh$_{el}$ and about 2.4 mg/kWh$_{el}$ (de Gouw et al., 2014). Another study reported (in 2013) the following SO_2 LCA emission intensities: 10-320 mg/kWh$_{el}$ range for natural gas power plants (of all kinds, not only the most efficient ones, i.e. the CCGTs), 30-6700 mg/kWh$_{el}$ range for coal-fired power plants, 3-38 mg/kWh$_{el}$ range for nuclear power plants (Turconi et al., 2013). At the time when Table 2 was originally computed (in 2007), coal-fired power plants (of high SO_2 emission intensity) were still in use for electricity generation. In fact, for example, Belgium closed its last coal-fired power plant in 2016 and was the seventh EU country to completely remove coal from its electrical mix (Asiaban et al., 2021). Therefore, SO_2 emissions from electrical radiators can be considered much lower than reported in this table. For example, considering the 2022 Belgian electrical mix (ELIA, 2023) and the maximum SO_2 emission factors for electricity generation reported by the European Topic Centre on Air and Climate Change (Fritsche and Rausch, 2009), the LCA SO_2 intensity of the 2022 Belgian electrical mix can be considered to only 77 mg/kWh$_{el}$, i.e. five times lower than the value reported in Table 2. In this calculation, the assumption that the 3.2 TWh electrical production referred to as 'Other' in the Belgian electrical mix (ELIA, 2023) entirely corresponds to the incineration of municipal waste with a SO_2 emission factor of 1220 mg/kWh$_{el}$, coming from the most SO_2 emitting waste incineration technology reported in the literature for China power plants (Chen and Christensen, 2010). This is a safe assumption (providing the worst SO_2 intensity for the Belgian electrical mix) as municipal waste incineration in Belgium corresponded only to 1 TWh per year in 2014 (Psomopoulos et al., 2017) or to 1.5 TWh in more recent years (Belgian Waste-To-Energy, n.d.) while other power plant technologies (hydropower, geothermal, solar-thermal, and solid biomass) are much cleaner, or are at worst similar (liquid biofuels) in terms of SO_2 emissions (Fritsche and Rausch, 2009). It is noteworthy that the Belgian nuclear electricity SO_2 emission factor has not been reported by the considered reference, i.e. the European Topic Centre on Air and Climate Change (Fritsche and Rausch, 2009). However, this reference still reported the nuclear electricity SO_2 emission factor in France (Belgian's neighbouring country), which was considered in this study to compute the LCA SO_2 intensity of the Belgian electrical mix.

Table 3.
Combustion only and Life Cycle Assessment (LCA) NO_x emission level reported from Energie+ (Energie+, 2007), which is a website developed by the University of Louvain-la-Neuve and the Energy Department of the Walloon Region, in Belgium. It is noteworthy that the electrical radiator emission factor has been established based on (and is therefore relevant for) the Belgian electrical mix.

Space-heating appliance	NO_x range (source from 1998: Electrabel-SPE – combustion only) mg/kWh$_{LHV}$	NO_x (source from 2007: Fondation Rurale de Wallonie - combustion only) mg/kWh$_{th}$	NO_x (source accessed in 2007: Gemis 4.5 - complete LCA cycle) mg/kWh$_{th}$
Old oil-fired boiler	up to 200	Unavailable	Unavailable
Non-Low NO_x oil-fired boiler	150 – 180	144	244
Low NO_x oil-fired boiler	90 – 120	Unavailable	Unavailable
Old gas boiler	150 – 200	Unavailable	Unavailable
Atmospheric gas boiler	100 – 180	Unavailable	Unavailable
Modulating gas condensing boiler	20 – 90	144	140
Electrical radiators (Joule heating)	420[a]	Unavailable	459
Old log wood boiler	Unavailable	180	Unavailable
Modern log wood boiler	Unavailable	151	235
Wood chip boiler (wood chips)	Unavailable	162	Unavailable
Condensing wood boiler (pellets)	Unavailable	Unavailable	344

[a] Considering the average Belgian electricity generation efficiency of 38% in 1998. Following the same methodology (and references) as conducted in Table 2 to establish the SO_2 intensity of the current Belgian electrical mix, the LCA NO_x intensity of the current Belgian electrical mix can be considered to be only 90 mg/kWh$_{el}$ or less, i.e. also about five times lower than reported in Table 3.

2.4 Pollutant emissions of residential fuel cells

A specific background study has been performed regarding the SO_2, NO_x, and/or CO emissions of residential fuel cells, and its results have been presented in Table 4. As it can be observed, there is only a very small number of works that provide information about the SO_2, NO_x, and/or CO emissions of residential fuel cell systems. In addition, in the consulted literature, the experimental emission measurement campaigns are seldom detailed (in terms of sensors or procedure). Pollutant emissions figures are even often reported without any references or are reproduced from the manufacturer's datasheets. It is noteworthy that pollutant emissions are never given by the same reference both in ppm (concentration) and in mg/kWh (intensity per unit of energy), which impedes the comparison between sources. These limitations therefore strengthen the interest of this experimental research.

Table 4.
NO_x and SO_x (or SO_2) emissions of fuel cell systems reported in the literature.

Technology	NO_x	SO_x (or SO_2)	References	Comments
PEMFC	<1 ppm	<1 ppm	(de Bruijn, 2005) Same fuel cell and figures reported in another study: (Srinivasan and Miller, 2006)	Figures seem to have originated from a document written by the manufacturer (original sources not available). Figures therefore not verified in an available documented experimental study.
Residential fuel cells in general. Unspecified.	<5 ppm	Not disclosed	(Krist, 1999)	Figure undocumented in the reference.
Fuel cells in general (residential market included). Unspecified.	< 9.07 mg/kWh[a]	Not disclosed	(Fouad et al., 2007)	Figure undocumented in the reference. The micro-cogeneration market is mentioned by the reference so the reported figure can be assumed to apply to residential fuel cells.
PEMFC	27.22 mg/kWh[a]	Not disclosed	(Shipley and Elliott, 2004)	Figure documented in the reference as: 'Source: Personal Communication with Joel Bluestein 2002'. The residential or micro-cogeneration markets have not been mentioned regarding this figure.
SOFC	4.54 mg/kWh[a]	2.27 mg/kWh[a]	(Shipley and Elliott, 2004)	Figure documented in the reference as: 'Source: Personal Communication with Joel Bluestein 2002'. The residential or micro-cogeneration markets have not been mentioned regarding this figure.
PAFC (Phosphoric Acid Fuel Cell)	13.61 mg/kWh[a]	2.72 mg/kWh[a]	(Shipley and Elliott, 2004)	Figure documented in the reference as: 'Source: Personal Communication with Joel Bluestein 2002'. PAFCs are not considered for the residential market (Nicolas Paulus, 2024b). 200 kW_{el} applications are indeed reported in the reference.
MCFC (Molten Carbonate Fuel Cell)	22.68 mg/kWh[a]	Not disclosed	(Shipley and Elliott, 2004)	Figure documented in the reference as: 'Source: Personal Communication with Joel Bluestein 2002'. MCFCs are not considered for the residential market (Nicolas Paulus, 2024b). 250-2000 kW_{el} applications are indeed reported in the reference.

[a] Supposedly expressed in mg/kWh_{th} or mg/kWh_{LHV} (rather than in mg/kWh_{el}) as it is usually considered in literature (and as it is the case in Table 2 and Table 3).

CO emissions are even more rarely reported. The only available figure is 10 ppm for a 20 MW_{el} Molten Carbonate Fuel Cell (MCFC), i.e. a figure reported to be similar to the emissions of gas turbines (Karvountzi and Duby, 2008). However, MCFC is not a residential fuel cell technology (see Table 4). It is noteworthy that the same MCFC fuel cell is reported in the consulted study to feature 0.03 ppm of NO_x, i.e. an order of magnitude lower than gas turbines and two orders of magnitude lower than reciprocating engines (Karvountzi and Duby, 2008). Regarding NO_x, those order of magnitudes has been confirmed in another study (Shipley and Elliott, 2004), which however explicitly reports that the considered reciprocating engines do not feature any NO_x-reducing catalyst in the exhaust.

2.5 Methane slip in natural gas-fed fuel cells

It should be mentioned that methane slip (or slippage), i.e. 'unburnt' methane emissions are sometimes mentioned in fuel cell literature. However, this term is usually rather used not for the methane content in the flue gases but

for the methane slipping from the reformer to the stack (to the anode of the fuel cell stack) if the fuel cell is not directly fed by hydrogen but by natural gas or other hydrocarbons (Aguiar et al., 2004; Chartrand, 2011; Kee et al., 2008).

Regarding Solid Oxide Fuel Cells (SOFCs), their high operating temperature fuel flexibility allows them to directly use methane (and other hydrocarbons) as fuel onto the stack anode, as it has been reported in Table 1. In addition, in the case of commercialized mCHP SOFC systems, existing studies of exhaust gases reported in the literature have shown that there is no or negligible methane slip (Payne et al., 2009). It has in fact been reported that the 'operation of the stack' is at a temperature between 700 and 800°C, which 'enables the internal reforming to proceed with negligible methane slip', which maximizes the amount of fuel available for the electrochemical process (Payne et al., 2009). Increased internal SOFC temperatures have indeed been reported to significantly reduce methane slip/emissions in exhaust gases (Wagner et al., 2002). Furthermore, specific SOFC literature confirms that, when operated on natural gas, SOFC do not have problems with methane slip in exhaust gases (Baldi et al., 2020; Kistner et al., 2021).

Regarding Proton Exchange Membrane Fuel Cells (PEMFCs), their stack relies on high-purity H_2 fuel (Urdampilleta et al., 2007), which implies reforming processes if the fuel cell is fed by natural gas or other hydrocarbons (Bang et al., 2022; Rabiu et al., 2012), as it has been inferred in Table 1. In fact, CH_4 concentrations up to 20 ppm downstream of the fuel processor and upstream of the fuel cell stack (anode) have been reported not to affect the power generation performance (Minei et al., 2020). However, an afterburner is usually implemented with PEMFC systems fed by natural gas in order to ensure the (complete) utilization of the unreacted fuel, which mainly consists of CH_4 and H_2 (Rabiu et al., 2012; Schumann et al., 2008), simultaneously providing the necessary heat to the reforming processes (Rabiu et al., 2012).

For those reasons and also because of the unavailability of dedicated CH_4 sensors to place in the exhausts of the systems in the experimental studies performed in this study, potential unlikely methane emissions of fuel cell mCHP systems have not been considered from here onwards.

3. Material and methods

3.1 Tested systems

3.1.1 PEMFC hybridized to a gas-condensing boiler

The PEMFC is not a standalone unit. It is hybridized to a gas-condensing boiler and to a Domestic Hot Water (DHW) tank. It is fed by natural gas and is designed to cover all the heat demands, including DHW, of residential houses and to participate locally in the electrical production. This particular system exists in several versions all based upon the same PEMFC module of nominal constant power of $0.75kW_{el}$ (and $1.1kW_{th}$) and the same 220L DHW tank. The only module that may vary is the gas boiler which is supposed to ensure peak heat demands. Indeed, it exists in four rated power versions from 11.4 to $30.8kW_{th}$, depending on thermal needs (Paulus and Lemort, 2023a). The heat rate output of the field-test system considered in this study is rated at 24.5 kW_{th} and is located in Huy, in Belgium. The system's architecture is presented in Figure 2, which does not show the double-walled chimney used for both the air inlet and flue gas exhaust (Lichtenegger et al., 2015). The PEMFC gas boiler hybrid system (from the laboratory facilities) is presented in Figure 3(a) without its front panel cover. Main datasheet characteristics are presented in Table 5.

Table 5.

PEMFC gas boiler hybrid expected targets. Publicly available data from the datasheet (Paulus and Lemort, 2023a).

Datasheet figures	Values
Maximum electrical production a year	$6200kWh_{el}$
Fuel cell rated electrical and thermal power as defined by EN 50465 (Dávila et al., 2022a)	$0.75kW_{el}$ & $1.1kW_{th}$
Electrical fuel cell efficiency	37% (LHV)
Max global Fuel cell efficiency	92% (LHV)
Max boiler efficiency (at rated power) [a]	108.7% (LHV)
NO_x class 6 (European Commission, 2021)	7.2 mg/kWh
Size without chimney (Height x Width x Depth)	1800 mm x 595 mm x 600 mm

[a] Considering High Heating Value (HHV) to Low Heating Value (LHV) ratio of 1.1094 (Jedlikowski et al., 2020).

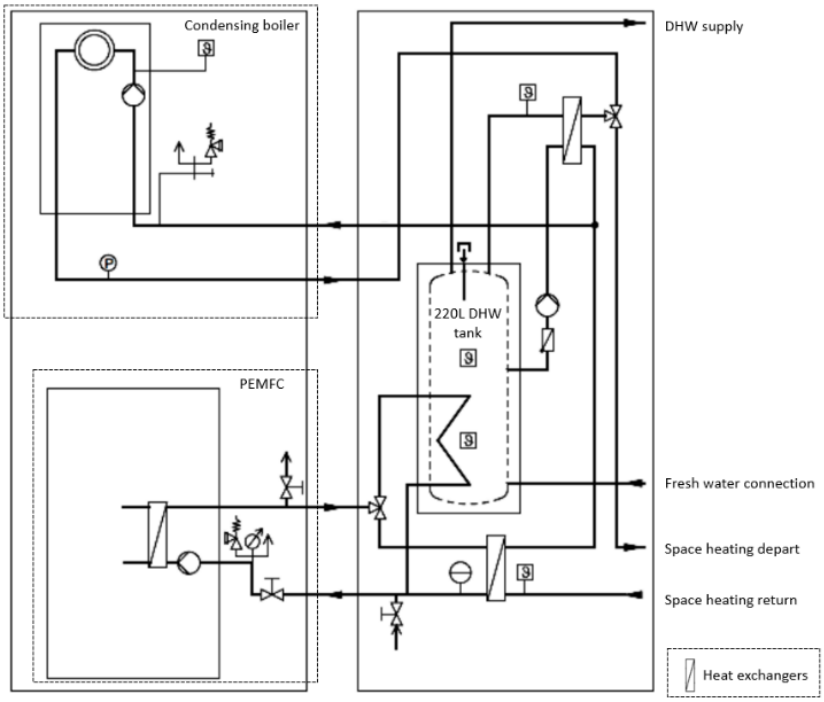

Figure 2. PEMFC system's architecture, including two heat exchangers, several 3-way valves, several circulators, the gas condensing boiler, and the DHW tank. Reproduced from reference (Paulus et al., 2022a).

The complete system's behaviour is heat driven. Its PEMFC has not been designed to be driven by the electrical demand and it is preferable that it runs as long as possible. It includes a methane reforming apparatus to feed the fuel cell stack with clean hydrogen and requires an automated fuel cell shutdown recovery procedure of 2.5 hours at least every two days to handle some reversible aging processes (Paulus et al., 2024). For further information, this system has been quite exhaustively studied in other publications (Dávila et al., 2022a; Paulus et al., 2024, 2022a, 2022b; Paulus and Lemort, 2023b, 2022b).

(a) (b)

Figure 3. Tested fuel cell mCHP systems in the laboratory facilities. (a) PEMFC; (b) SOFC.

3.1.2 SOFC

The studied SOFC is also fed by natural gas. It is designed to provide 1.5 kW_{el} of nominal output power with a high announced LHV electrical efficiency of 60%, along with a heat recovery of 0.6 kW_{th} representing a LHV thermal efficiency of up to 25% (Paulus and Lemort, 2022a). The output power can be modulated down remotely (by the manufacturer, upon the owner's request) as wanted in the 0.5 - 1.5 W_{el} range, affecting those announced efficiencies. It is not advised to completely shut it down because thermal cycles affect its durability and because

startup operations are long and have been reported in the user manual to last up to 30 hours (Paulus and Lemort, 2023c).

Discarding its chimney, the system is approximately the same size as a dishwasher, as it can be seen in Figure 3(b). Its internal schematics have not been disclosed but have been discussed in a previous publication (Paulus and Lemort, 2022a), based on observations of the system and cogeneration SOFC literature. Amongst other particularities, the reforming process of the inlet natural gas (into hydrogen) is not only internal (Paulus and Lemort, 2022a). Indeed, it does not only occur directly at the anode, onto the stack, with the high operating temperatures occurring with that fuel cell technology (Aguiar et al., 2004), but it also uses an external steam reformer upstream of the stack, called 'pre-former' (Paulus and Lemort, 2022a). For information, the newer version of this system is stated by the manufacturer as belonging to class 6 in terms of NO_x (D2SERVICE, 2019), according to EN 15502-1 (European Commission, 2021). This is the most stringent NO_x emission class, which corresponds to a limit of 56 mg/kWh based on natural gas high heating value (Bălănescu and Homutescu, 2018), i.e 62 mg/kWh based on natural gas low heating value (Jedlikowski et al., 2020), as it has been reported in Table 6. The exact emission levels have however not been reported, to the knowledge of the authors.

Table 6.
NO_x emissions classes for gas condensing boilers according to EN 15502 (European Commission, 2021) and for gas absorption heat pumps according to EN 12309 (European Commission, 2014). The NO_x emissions limits are identical. Reproduced from references (Venfield and Brown, 2018; VHK for the European Commission, 2019).

NO_x class	EN 15502 NO_x concentration limit Low heating value-based	EN 15502 NO_x concentration limit High heating value-based	EN 12309 NO_x concentration limit Low heating value-based
1	260	234 [a]	260
2	200	180 [a]	200
3	150	135 [a]	150
4	100	90 [a]	100
5	70	63 [a]	70
6	62 [a]	56	Unavailable

[a] Considering High Heating Value (HHV) to Low Heating Value (LHV) ratio of 1.1094 (Jedlikowski et al., 2020).

3.1.3 Gas condensing boiler

The tested mural gas condensing boiler dates from 2005 and is quite classical. Its identification name is 'Buderus Logamax plus GB142-45' and it can provide up to 45 kW_{th} (that can be modulated down to 30%). It can provide heat to an optional DHW tank but cannot provide instantaneous DHW directly as it has only one hydraulic inlet and one hydraulic outlet (used in close circuit configurations). The emissions of CO and NO_x are reported by the manufacturer respectively to 15 mg/kWh and 20 mg/kWh (Buderus, 2011).

3.1.4 Euro 6 diesel vehicle

The tested vehicle is a 4-year BMW X1 sDrive18d that is proper maintenance and had 111210 kilometres on the odometer at the moment of the test. Its four-stroke engine has four cylinders and represents a displacement of 1995cm³. Net power is 100 kW at 4000 rpm. The certificate of conformity presents average emissions on the New European Driving Cycle (NEDC) for CO and NO_x respectively of 86.8 mg/km and 19.2 mg/km. Maximum Real Driving Emissions (RDE) NO_x emissions are reported to be equal to 168 mg/km. Considering an effective consumption of 6L per 100 km (according to the dashboard of the vehicle), considering a diesel LHV of 43.51 MJ/kg and a density of 827 kg/m³ (Parravicini et al., 2020), those emissions correspond respectively to 145 mg/kWh (average CO emissions on the NEDC), 32 mg/kWh (average NO_x emissions on the NEDC) and 280 mg/kWh (maximum Real Driving Emissions NO_x). They are relative to the diesel LHV input to the engine.

3.1.5 Gas absorption heat pump

It is noteworthy that another uncommon commercial natural gas space heating appliance was tested with the same sensors as the previously described systems. Indeed, similar pollutant tests were conducted in a laboratory environment over a gas absorption heat pump named 'Robur K18 Simplygas' from 2019. The system is based on the Water-Ammonia absorption cycle using outdoor air as renewable energy source (low-temperature heat source) and natural gas combustion as high-temperature heat source; the delivered hot water is the medium-temperature heat sink. This heat pump shows a nominal heating output of 18,9 kW with an outdoor temperature of 7°C and delivery temperature of 35°C, and its datasheet announces a 169% low heating value efficiency in those conditions (Robur, 2022). It is designed for domestic hot water and space heating production. Its working principle and performance analysis have been reported in a previous study (Dávila et al., 2022b).

For information, the newer version of this system is stated by the manufacturer as belonging to class 5 in terms of NO_x (Robur, 2020), according to EN 12309-1 (European Commission, 2014). The exact emission levels, expected

to be below the limit of 70 mg/kWh based on natural gas low heating value according to Table 6, have however not been reported to the knowledge of the authors.

3.2 Measurements device

To perform the pollutants emissions analyses of the tested systems, the same portable combustion analyser meter was used. It is called 'Multilyzer STx' and is shown in Figure 4 whereas its specifications are shown in Table 7.

It measures CO, NO, NO_2, and SO_2 in ppm, whereas O_2 and CO_2 concentration levels are expressed in percentage (by volume). Carbon monoxide sensors generally have a significant cross-sensitivity to hydrogen, meaning that the real carbon monoxide concentration can be overestimated if hydrogen is present as well in the tested gas sample (Hall et al., 2021). Therefore, as presented in Table 7, the 'Multilyzer STx' combustion analyser portable meter has implemented a hydrogen compensation for its carbon monoxide measurements. However, it can already be stated that, for the tests conducted in this study, there were not any significant differences between the signals provided by the sensor for the CO concentration measurement and for the hydrogen compensated CO measurements, indicating that hydrogen levels in the exhaust appliances were always negligible.

Figure 4. 'Multilyzer STx' combustion analyser portable meter.

Table 7.
Specifications of the 'Multilyzer STx' combustion analyser portable meter. Publicly available data published by the manufacturer (AFRISO-EURO-INDEX Group, 2019).

Pollutant	Range	Accuracy	Resolution
NO	0 - 5000 ppm	± 5 ppm (< 50 ppm) ± 5% reading (> 50 ppm)	1 ppm
NO_2	0 - 500 ppm	± 10 ppm (< 50 ppm) ± 10% reading (> 50 ppm)	1 ppm
SO_2	0 - 5000 ppm	± 10 ppm (< 200 ppm) ± 5% reading (> 200 ppm)	1 ppm
CO (hydrogen compensated)	0 - 10000 ppm	± 5 ppm (< 50 ppm) ± 5% reading (> 50 ppm)	1 ppm
O_2	0 - 21 % vol.	± 0.2% vol.	0.1% vol.
CO_2 (calculated from O_2 level)	0 % vol. up to $(CO_2)_N$ which depends on fuel type, see Equation (1)	± 0.2% vol.	0.1% vol.
Gas temperature	0 - 1150 °C	± 1 °C (0 - 300°C) ± 1% reading (> 300°C)	0.1 °C

It can be interesting to compare fixed continuous pollutant analysers to portable analysers, such as the 'ENERAC Model 500' (Edelblute et al., 2015), or such as the 'Multilyzer STx' used in this study and presented in Table 7 (which present both similar performances). For example, as many others, a study conducted on a combustion

engine test bench used the very common 'AVL Digas 444N' gas analyser and established its performance, as reported in Table 8 (Balamurugan and Nalini, 2014). Comparing Table 7 and Table 8, it can be established that the measuring range of both sensors is quite similar, except for CO, which is an order of magnitude higher for the fixed sensor, considering ppm vol. and ppm values similar by the assumption of ideal gases behaviors (through the ideal gas law). This increased range has however as consequence that its CO measuring resolution is an order of magnitude worse than for the portable sensor used in this study. With the comparison of both the fixed and portable multi-gas analysers of Table 7 and Table 8, it can be established that there are no benefits of using a fixed measuring device instead of a portable one in terms of resolution, measuring range, and especially in terms of accuracy (which is even often worse with the fixed multi-gas sensor of Table 8 than for the one used in this study).

Table 8.
Specifications of the 'AVL Digas 444N' combustion analyser fixed meter. Reproduced and adapted from references (AVL, 2021; Balamurugan and Nalini, 2014). It is noteworthy in the datasheet of the 'AVL Digas 444N' sensor currently available, some of the measuring ranges have slightly been increased (AVL, 2021). Similarly, in another study, the accuracy regarding the O_2 measurements has been established to ±1% vol. (Patnaik et al., 2016), but this is still not better than for the 'Multilyzer STx' used in this work (as reported in Table 7).

Pollutant	Range	Accuracy	Resolution
NO_x	0 – 5000 ppm vol.	±10% reading	1 ppm vol.
CO	0 - 10 % vol. (0 – 100 000 ppm vol.)	±0.03% vol.	10 ppm vol.
O_2	0 - 22 % vol.	±5% vol.	0.01% vol.
CO_2	0 – 20 % vol.	±0.5% vol.	0.1% vol.

However, when considering only the NO_x measurements (and not muti-gas analysers), some fixed continuous analysers feature truly enhanced resolution (and, to a lesser extent, accuracy). For example, the 'Serinus 40', the 'Thermo Scientific Model 42i', the 'API T200' and the 'API T500u' all exhibit resolutions of 0.4 ppb (for the '42i' in its selectable 500 ppb range) or 0.5% of reading (for the other sensors), which, depending on their range, can either reach the maximum values of 5 ppb (for the 'API T500u') or 100 ppb (for the 'Serinus 40' and the 'API T200'). Based on their reported linearity of ±1% full scale, it can be assumed that the relative accuracy of those sensors is also enhanced compared to the portable sensor used in this study. The range of those sensors is however much more limited (as they are primarily designed for ambient air analyses rather than combustion analyses), i.e. up to 100 ppm for the 'Thermo Scientific Model 42i', up to 20 ppm for the 'Serinus 40' and the 'API T200', or even up to 1 ppm for the 'API T500u'. These sensor performances have been reproduced from consulted studies and/or from the respective datasheets (acoem, 2022; Landis and Edgerton, 2024; Rana et al., 2019; Teledyne API, 2021a, 2021b; Thermo Scientific, 2021).

A commonly used NO_x combustion fixed analyser with a similar range as the one used in this study (yet still five times lower, i.e. 1000 ppm) is the '4000VML' (Signal Instruments, 2006). It is indeed an interesting sensor because it also presents a linearity of ±1% full scale, i.e. a figure that can be closely linked to the accuracy and which is therefore significantly increased compared to the portable sensor used in these experiments (Signal Instruments, 2006). Noticeably, in combustion analyses (fixed) test bench, it has been reported to have been combined with the 'AVL Digas 444N' sensor already presented in Table 8, to compensate for this latter's poor NO_x measurements performance (Solomon et al., 2020).

Regarding SO_2 measurements, a commonly used fixed sensor worth citing is the 'Serinus 50', exhibiting a measuring range of up to 20 ppm, a resolution of 0.5% of reading, and a linearity of ±1% full scale (acoem, 2023; Park et al., 2021; Vrekoussis et al., 2022). Compared to the portable sensor used in this study, the range is significantly reduced while the resolution and accuracy can be assumed significantly increased.

To summarize this fixed-to-portable sensor comparison, for low pollutant levels (which, according to Table 4 can be expected with fuel cells), it could indeed be beneficial in terms of accuracy and resolution to use fixed continuous acquisition bays. However, in the case of this study, a lot of the tests had to be conducted in field-test applications (as it will be detailed in the *Testing procedure* section) and the choice of a portable sensor was mandatory.

3.3 Conversion of ppm to mg/kWh

As demonstrated in the previous section, literature on space heating appliances pollution levels is quite rare and pollutant emissions are regularly reported in terms of concentration, i.e. in ppm (McDonald, 2009), or in terms of intensity, i.e. in mg/kWh (Energie+, 2007). However, it is quite rare for both pieces of information to be provided. In this case, the pollutant emissions measurements are provided by the metering device in ppm (see Table 7) whereas, for comparison purposes, it would be more meaningful to express them in terms of mg/kWh. Indeed, Table 3 for example reports from literature the NO_x emission levels of several space heating appliances in

mg/kWh. In addition, as reported in the *Tested systems* section, the datasheets of the tested space heating appliances only express the emissions in terms of mg/kWh. Therefore, to use those figures as references for this study, the emission measures performed in this work must be converted from ppm to mg/kWh.

For natural gas appliances, this can be performed thanks to Equation (1) for carbon monoxide emissions (European Commission, 2021):

$$CO_{(mg/kWh)} = 1.074 \times CO_{(ppm)} \times \frac{(CO_2)_N}{(CO_2)_M} \quad (1)$$

Where $CO_{(mg/kWh)}$ is the carbon monoxide emissions level per unit of energy (kWh) that must be established for the studied combustion test; $CO_{(ppm)}$ is the measured carbon monoxide concentration at the exhaust of the system during the combustion test (in ppm); $(CO_2)_M$ is the measured carbon dioxide concentration at the exhaust of the system during the combustion test (in %) and $(CO_2)_N$ is the maximum carbon dioxide concentration of the dry, air-free, combustion products (in %), which depends only on the natural gas type that is fed to the studied system during the combustion. $(CO_2)_N$ is equal to 11.7% for G20 natural gas and 11.5% for G25 natural gas (European Commission, 2021).

Indeed, in Belgium (Paulus and Lemort, 2023d), as in France or Germany (Bruijstens et al., 2008), natural gas comes from different sources, which implies different gas compositions and different HHV and leads to the appellations 'lean' and 'rich' gas, respectively for the natural gas source providing the lower and the higher HHV (Haeseldonckx and D'haeseleer, 2007). Lean gas is also called 'L-gas' (CREG, 2018), 'type L' gas (Paulus and Lemort, 2023d) or G25 (Bruijstens et al., 2008) whereas rich gas is also called 'H-gas' (CREG, 2018), 'type H' gas (Paulus and Lemort, 2023d) or G20 (Bruijstens et al., 2008). The type of gas provided on the grid only depends on the localization of the delivery point. All lean gas deliveries are supposed to be progressively replaced (in Belgium) by 2030 by rich gas deliveries (CREG, 2018).

As reported in the previous section, $(CO_2)_M$ and $CO_{(ppm)}$ are provided by the meter used in this work. Also, in Equation (1), the 1.074 constant is the unit conversion coefficient related to CO emissions from natural gas appliances (Zlateva et al., 2020).

Similarly, ppm to mg/kWh conversion for NO_x emissions is obtained thanks to Equation (2) for natural gas appliances (European Commission, 2021) :

$$NOx_{(mg/kWh)} = \frac{\left(C_g \times NOx_{(ppm)} \times \frac{(CO_2)_N}{(CO_2)_M}\right) - 0.85(20 - T_m) + \frac{0.34(h_m - 10)}{1 - 0.02(h_m - 10)}}{\left(1 + \frac{0.02(h_m - 10)}{1 - 0.02(h_m - 10)}\right)} \quad (2)$$

Where $NOx_{(mg/kWh)}$ is the nitrogen oxide emissions level per unit of energy (kWh) that must be established for the studied combustion test; C_g is the unit conversion coefficient related to NO_x emissions from natural gas appliances (Bălănescu and Homutescu, 2017) and is equal to 1.764 for G20, i.e. rich gas, or 1.767 for G25, i.e. lean gas (European Commission, 2021); $NOx_{(ppm)}$ is the sum of the measured nitrogen dioxide and nitric oxide concentrations at the exhaust of the system during the combustion test (in ppm); $(CO_2)_N$ and $(CO_2)_M$ have already been described for Equation (1); T_m is the temperature of the outdoor air used for the combustion (in °C) and h_m is the absolute humidity of the outdoor air used for the combustion (in g of water per kg of dry air). h_m is the only variable of Equation (2) that is not provided by the combustion analyser meter (see Table 7). By assimilating inlet air to humid air of relative humidity between 40 and 80%, at atmospheric pressure and at the T_m temperature, h_m can be approximated with the Engineering Equation Solver (EES) software. It is worth mentioning regarding Equation (2) that the allowable ranges for T_m, h_m $NOx_{(mg/kWh)}$ and are respectively 15 - 25 °C, 5 - 15 g of water per kg of dry air, and 50-300 mg/kWh. However, industrial partners in this work advise using Equation (2) anyway even if some parameters are out of those ranges.

The European standard from which Equation (1) and Equation (2) are deduced (European Commission, 2021) unfortunately does not provide any information about SO_2 emissions conversion. Fortunately, another reference (TSI Incorporated, 2004) provided Equation (3), which has been reported to be relevant not only for SO_2 but also for CO and NO_x emissions, giving similar conversion results, at least in its documented allowable range, respectively to Equation (1) and Equation (2).

$$PEI_{(mg/kWh)} = F \times PEC_{(ppm)} \times \frac{20.9}{20.9 - (O_2)_M} \quad (3)$$

Where $PEI_{(mg/kWh)}$ is the pollutant emissions intensity, i.e. the emission level per unit of energy (kWh) that must be established for the studied combustion test; F is an emission rate conversion factor that depends on the pollutant (and the type of fuel) and that is given in Table 9, $PEC_{(ppm)}$ is the measured pollutant emissions concentration at the exhaust of the system during the combustion test (in ppm) and $(O_2)_M$ is the measured oxygen concentration at the exhaust of the system during the combustion test (in %). Equation (3) has the particularity to consider O_2 concentration (in %) in the exhaust whereas Equation (1) and Equation (2) rely on CO_2 concentration (in %).

Similar conversion equations for diesel engines have not been reported in this paper but can also be found in the literature (Pilusa et al., 2012).

Table 9.

Natural gas *F* coefficients for Equation (3) depending on the pollutant type (TSI Incorporated, 2004).

Pollutant	*F* mg/(kWh-ppm)
CO	0.974313
NO_x	1.608389
SO_2	2.242466

3.4 Testing procedure

The end of the probe of the 'Multilyzer STx' must be placed at the centre of the exhaust gas chimney (or tailpipe) and the probe axis can either be oriented in the perpendicular plane of this chimney (or tailpipe) or parallel to it (if the measurements are conducted at the exit of the chimney/tailpipe). The probe disposes of a conical adjustable mechanical stop to ensure the correct probe depth to the centre of the chimney (see Figure 4).

The studied PEMFC system, which is composed of a PEMFC stack hybridized to a gas condensing boiler (as seen in the *Tested systems* section), has the advantage of being equipped by design with a small, sealable access hole, fitted with a cap, directly at the exhaust of the system (in the first 5 cm of the chimney). There is thus no need for the PEMFC system to place the combustion analyser meter at the exit of the chimney, which access is very often difficult and potentially risky if it figures on the roof of the building. However, some measurements have still been taken at the exit of the chimney for comparison purposes (with the probe fully inserted in the chimney). Indeed, temperature (which varies all along the double-walled chimney that cools down the flue gases and heats the inlet air from outdoors) is not only known to influence the NO_x formation but also the NO-NO_2 equilibrium. This is especially the case in the near-post-flame zone (Bowman, 1975), i.e. close to the outlet of the system, but also in the atmosphere, i.e. close to the exit of the chimney, in the presence of Volatile Organic Compounds (Cheremisinoff and Young, 1977), which can be co-emitted in hydrocarbons combustion (Bowman, 1975).

The PEMFC hybrid system was tested in two separate modes: with only the PEMFC turned on and with only the gas condensing boiler turned on. This system, installed in 2019, was tested in a field-test application (in a real house) in Huy (in Belgium). At the moment of the tests, the whole machine has been functioning for about 15000 hours, but its integrated fuel cell has only been producing electricity for about 5500 hours. It is worth mentioning that another machine of this system, which was perfectly new, was tested in a laboratory environment (as it will be seen in the results reported in Figure 6).

The studied mCHP SOFC system does not involve any hole in its chimney by design. However, since one machine of this system was tested in laboratory facilities, a hole was manufactured at a chimney height of 50 cm (above the system flue gases outlet). This was also the case for the tested gas absorption heat pump (which was tested in steady state, at its rated power). The SOFC tested in the laboratory was used for two pollutant test campaigns (conducted at minimum and intermediate electrical power output, i.e. 500 W_{el} and 1000 W_{el}). This machine, installed in 2021, had already been functioning for about 6000 hours before being tested. In the laboratory facilities, the return temperature of the heat recovery circuit, which affects the exhaust gas temperature, could be controlled (Paulus and Lemort, 2023c). For the other pollutant test campaign (at full-rated electrical power output, i.e. 1500 W_{el}), the combustion analyser meter was placed in another configuration. It was indeed positioned at the exit of the chimney (and fully inserted in it) since this campaign was performed on another SOFC machine (with the same reference) in a field-test application in Riemst (Belgium). At the moment of the pollutant measurements, this second machine, installed in 2017, has already been functioning for about 45000 hours.

As mentioned in the *Tested systems* section, another classical gas condensing boiler has been tested (only at the exit of its chimney, with the probe fully inserted in it). This system was tested in a field-test application in Riemst (Belgium).

At last, the Euro 6 diesel vehicle was tested at the exit of both of its tailpipes. The probe of the sensor could be oriented parallel to the tailpipe, so it has either been fully inserted in the tailpipe (about 35 cm before its exit) or only inserted over about 15 cm. The purpose was to see the changes in the exhaust gas temperature and their impact on the pollutant measurements. It is worth mentioning that the car engine was tested at idle (±850 rpm) and at 1500 rpm, but the clutch was always disengaged.

All the tests include a purge with clean air before starting the measurements. It is indeed a mandatory step requested by the 'Multilyzer STx' combustion analyser meter. At last, the sample time was always one second.

4. Results

All the tests may also have included other specificities in the way they have been conducted and those are reported accordingly in Table 10 along with the pollutant emissions results.

Firstly, for the tests conducted in this study, there were not any significant differences between the signals for the CO concentration measurement and for the hydrogen-compensated CO measurements provided by the sensor (as mentioned in the *Measurements device* section), indicating that hydrogen levels in the exhaust appliances were always negligible. Thus, only the CO measurements have been reported in Table 10 and in the rest of this work.

The results reported in the first row of Table 10, i.e. conducted for the studied PEMFC gas boiler hybrid system with only the fuel cell running, have been reproduced in Figure 5 for illustration purposes. It is interesting to point out that an inexplicable short CO peak of about 60 ppm is noticeable after about 25 min of measurements, with the fuel cell running constantly (without any change operated to its control by the user or technicians). It will later on be seen in Figure 6 that a similar CO peak also occurs at the fuel cell startup of the same PEMFC gas boiler hybrid system, but in this case, the fuel cell was already running. However, it is likely to be related to an online (yet unidentified) recovery operation. Indeed, such PEMFC fuel cells are known to be very sensitive to impurities (as reported in Table 1) and many recovery mechanisms (conducted online or offline) can be associated with this fuel cell technology (Paulus et al., 2024).

Later in the acquisition signals (after about 47 min of measurements), Figure 5 also shows combined short NO, NO_2, and CO peaks that coincide with an elevation of temperature of the flue gases. Those peaks also coincided with a sudden increase in gas consumption (that was monitored for this field-test site) and it was concluded that it corresponded to an inexplicable startup (and shutdown) of the gas boiler of the system. In fact, over a quite longer pollutant test conducted on the PEMFC-gas boiler hybrid of the field-test site of Oostmalle reproduced on Figure 7, similar pollutant peaks have clearly been identified to startups and shutdowns of the gas boiler. Figure 7 indeed shows that the gas boiler embodied in the PEMFC hybrid system is exhibiting unwanted ON/OFF cycling behaviour. As inferred by the literature, this highly transient behaviour of the gas boiler is expected to decrease the overall efficiency of the system (Bennett and Elwell, 2020). Additionally, it is interesting to point out from Figure 5 and Figure 7 that, although NO_x peaks only occur at boiler startups, CO peaks occur both at boiler startups and shutdowns.

Also, it is strongly believed that the high level of hybridization between the fuel cell and the gas boiler (seen in Figure 2) is responsible for those many unexpected boiler startups and shutdowns and therefore prevents both sub-systems from operating as optimally and reliably as they would have as standalone units.

At last, as it is the case in all the tests conducted through this study, no SO_2 emissions could be measured.

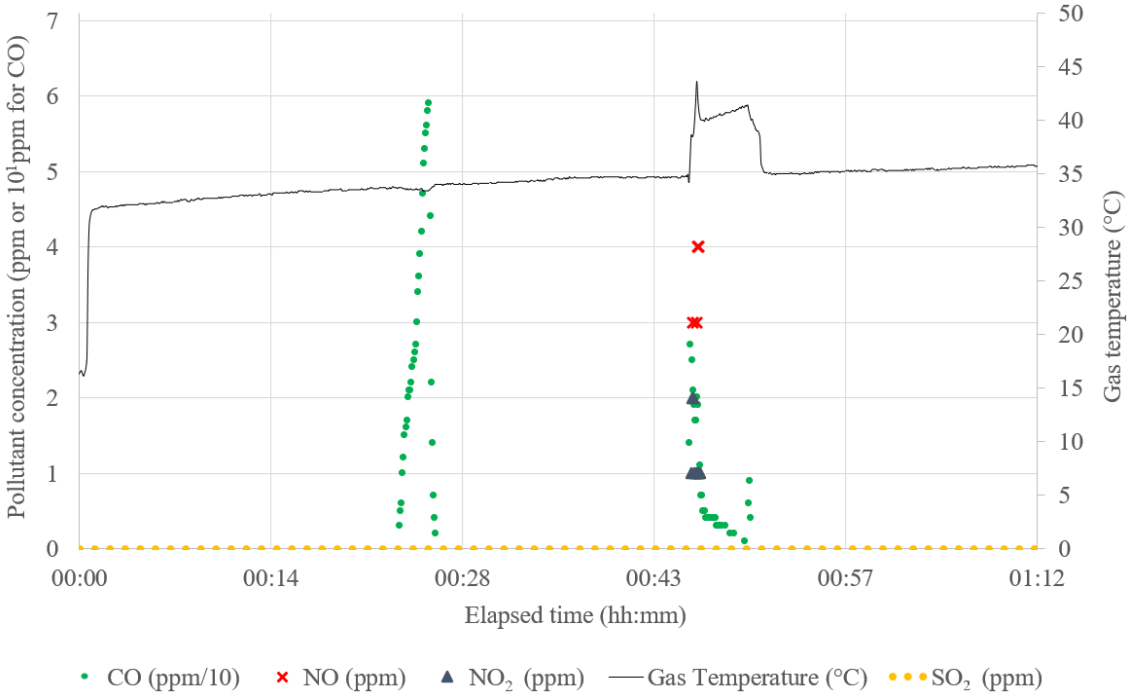

Figure 5. Pollutant measurements of the fuel cell (only) steady state phase of the PEMFC-gas condensing boiler hybrid system (performed at the field-test site in Huy). The gas temperature elevation at the start of the test corresponds to the moment when the probe of the pollutant sensor is moved from ambient (external) air to the exhaust chimney.

In addition, for information, a graphical example of another pollutant test (performed with the same sensor in a laboratory environment) is given in Figure 6 for the studied PEMFC system in its startup phase only (with the boiler turned off). In that test, no NO_x nor SO_2 could be measured. The startup phase (duration between the machine's startup initiated thanks to a thermal demand and the moment when the fuel cell starts producing electricity) takes about 7 min whereas the total duration to reach a steady state is about 15-20 min (gradually from 0 W_{el} to its nominal output power of 750 W_{el}). A CO peak of about 2 minutes, with a maximum at 55 ppm, can again be noticed at the beginning of the power and heat generation phase, probably due to transient behaviours of the internal reformer required for this PEMFC fed by natural gas (Paulus et al., 2024). The stepped behaviour of the CO_2 percentage measurement is explained by the resolution of the sensor and the fact that it is not directly measured but established by the combustion analyser from O_2 measurements (Table 7). However, the sudden CO_2 peak is probably an outlier as it could not be explained.

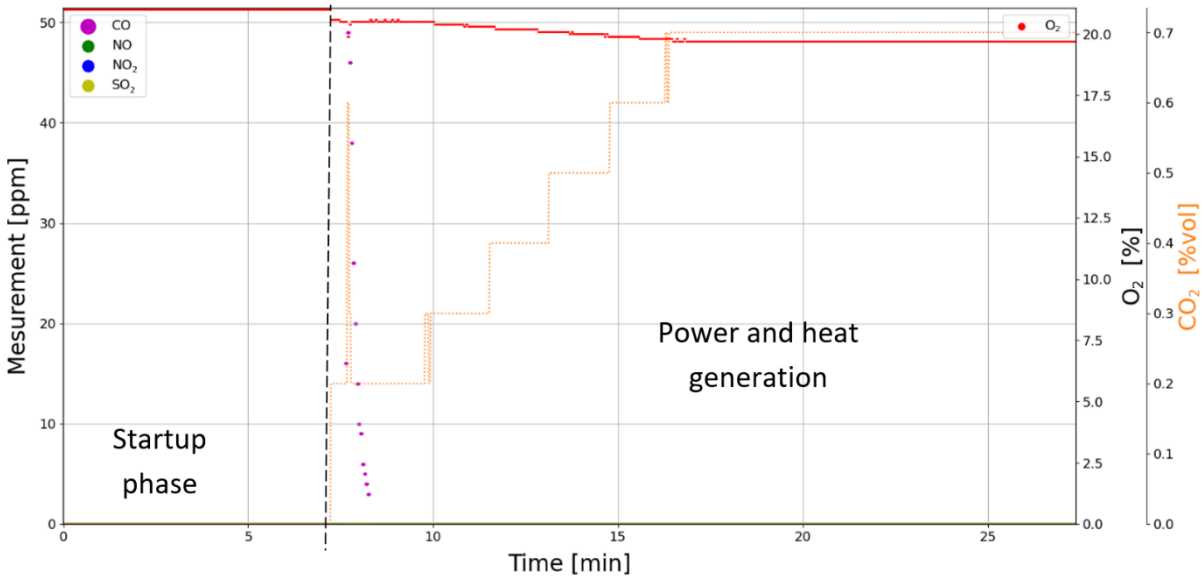

Figure 6. Pollutant measurements of the fuel cell (only) startup phase of the PEMFC-gas condensing boiler hybrid system (performed in a laboratory environment).

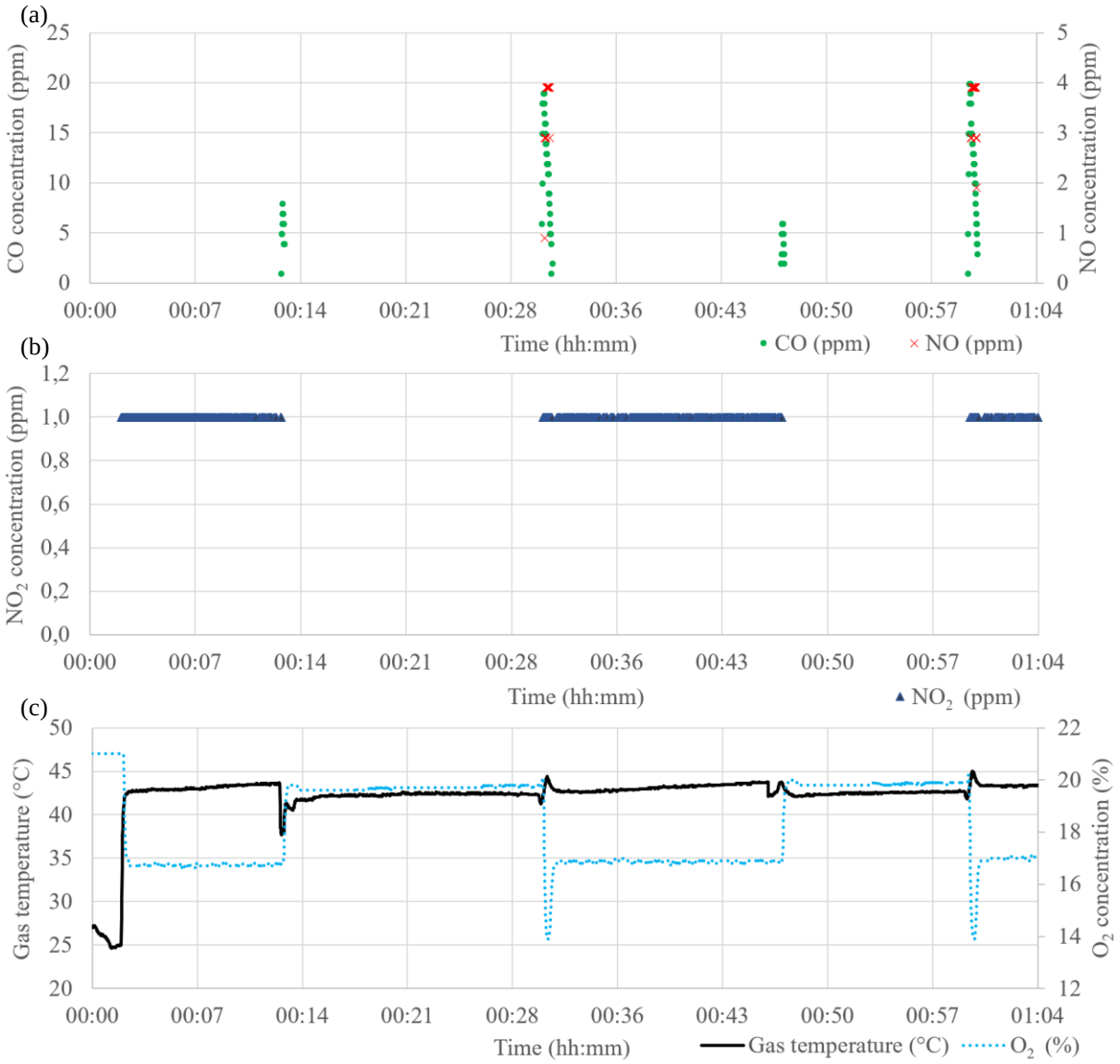

Figure 7. Pollutant measurements of the PEMFC-gas condensing boiler hybrid system (performed at the field-test site in Oostmalle). The fuel cell is always running and the sudden changes in the signals are related to the gas boiler being turned on and then turned off by the system itself (without any change operated to its control by the user or technicians). The gas boiler embodied in the system is therefore exhibiting unwanted ON/OFF cycling behaviour. The gas temperature elevation at the start of the test corresponds to the moment when the probe of the pollutant sensor is moved from ambient (external) air to the exhaust chimney. (a) CO and NO; (b) NO_2; (c) Associated O_2 concentration and gas temperature.

Table 10. Pollutant emissions measurements results (in all tests, the sensor indicated 0 ppm of SO_2 emissions).

Test and conditions	NO [a]	NO_2 [a]	CO [a]	Remarks
PEMFC hybrid system (**PEMFC only mode**) Measured on the field-test site in Huy without control on the return temperature (or on the exhaust gas temperature)	0	0	- Startup : short peak up to 55-60 ppm for 2 min (in total). Also measured in the laboratory (Figure 6). - Steady state : 0 but an unexplainable short peak similar to FC startup has been measured while the PEMFC was running (Figure 5).	- Boiler turned down by closing the radiator valves in the house - No difference in the pollutant measurement between the exit of the chimney (on the roof) and the exit of the system
PEMFC hybrid system (**condensing gas boiler only mode**) Measured on the field-test site in Huy without control on the return temperature (or on the exhaust gas temperature)	- Startup : peak up to 7 ppm for 5 min (in total) - Steady state : 0	- Startup : 3 ppm - Steady state : 3 ppm, i.e. 6.7 mg/kWh	- Startup : short peak up to 80 ppm for 30 sec (in total) - Steady state : 30 ppm, i.e. 40.7 mg/kWh	- Boiler turned on by opening the radiator valves in the house and setting a high-temperature setpoint on the thermostat; the PEMFC happened to be turned off, probably conducting a regeneration procedure (Paulus et al., 2024)
SOFC – 500 and 1000 W_{el} output Tested in laboratory with different heat recovery temperatures, i.e. different exhaust gases temperature (from 45°C to 25°C)	0	0	5 ppm (at 500 W_{el}), i.e. 28.3 mg/kWh 11 ppm (at 1000 W_{el}), i.e. 41.5 mg/kWh	- Return temperature of the heat recovery circuit has no influence on the pollutant measurements - Only steady state data (the system in supposed to be turned on continuously and the startup test was not conducted)
SOFC - 1500 W_{el} output Measured on the field-test site in Riemst with only one heat recovery temperature corresponding to 60°C of exhaust gases temperature	0	0	8 ppm, i.e. 17.0 mg/kWh	- Same SOFC reference as in the laboratory tests but a different machine) - Only steady state data (the system in supposed to be turned on continuously and the startup test was not conducted)
Classical gas condensing boiler - high DHW load (exhaust gases temperature of about 65°C at the exit of the chimney) Measured on the field-test site in Riemst	- Startup : peak up to 8 ppm for 2 min (in total) - Steady state : 5 ppm, i.e. 10.1 mg/kWh	- Startup : peak up to 4 ppm for 2,5 min (in total) - Steady state : 2 ppm, i.e. 4.1 mg/kWh	- Startup : peak up to 50 ppm for 2 min (in total) - Steady state : 10 ppm, i.e. 12.3 mg/kWh	- No remark
Classical gas condensing boiler – low-temperature space heating load (exhaust gases temperature of about 30°C at the exit of the chimney) Measured on the field-test site in Riemst	- Startup : Untested - Steady state : 0 ppm	- Startup : Untested - Steady state : 0 ppm	- Startup : Untested - Steady state : 8 ppm, i.e. 10.7 mg/kWh	- No remark
Gas absorption heat pump at rated power. Tested in laboratory.	- Steady state : 8 ppm, i.e. 16.9 mg/kWh	- Steady state : 12 ppm, i.e. 25.4 mg/kWh	- Steady state : 120 ppm, i.e. 153.7 mg/kWh	- No remark
Euro 6 Diesel Engine at idle, i.e. ±850 rpm (car in neutral)	- Startup : continuous increase for about 20 min up to 60 ppm - Steady state : 55 ppm, i.e. 238 mg/kWh (Pilusa et al., 2012)	0	- Startup : rapid increase for about 3 min to the 200-300 ppm range - Steady state : 200-300 ppm, i.e. 800-1200 mg/kWh (Pilusa et al., 2012)	- The probe must be fully inserted in the tailpipe to record pollutant emissions - There is no difference between the left and right tailpipes
Euro 6 Diesel Engine at 1500 rpm	- Startup : unavailable (engine already warmed up) Steady state : 40 ppm, i.e. 173 mg/kWh (Pilusa et al., 2012)	0	- Startup: unavailable (engine already warmed up) Steady state : 850 ppm, i.e. 3430 mg/kWh (Pilusa et al., 2012)	- The probe must be fully inserted in the tailpipe to record pollutant emissions - There is no difference between the left and right tailpipes

[a] Equation (3) has been used to convert ppm measurement into mg/kWh for steady state measurements only (of natural gas appliances). The similar conversion law for diesel engines comes from literature (Pilusa et al., 2012). Peaks and startups have highly transient dynamic behaviours both on the pollutant concentration and the O_2 percentage signal, making the ppm to mg/kWh conversion hazardous.

5. Discussion and limitations

None of the tested systems (PEMFC, SOFC, gas condensing boilers and Euro 6 diesel engine) showed any SO_2 emissions. This is either an indication of an issue with the SO_2 sensor or it proves the efficiency of the desulphurization treatment implemented in the natural gas process before it enters the grid (Paulus et al., 2024). In addition, both fuel cell systems include a desulphurizer in their respective fuel processors according to the consulted manufacturer's documentation. Regarding the diesel vehicle, the lack of SO_2 emissions could be explained by low sulphur content of diesel in the EU, limited to 10 ppm according to the EN 590:2009 regulation (European Commission, 2009). It could also be explained by the oxidation of SO_2 into SO_3 (not measured by the sensor) in the selective catalytic converter used in the exhaust of the engine to reduce NO_x emissions (Wade and Farrauto, 2012).

Both fuel cell systems (PEMFC and SOFC) do not show any NO_x emissions even if they involve high-temperature reforming processes (Paulus et al., 2024; Paulus and Lemort, 2022a). Oppositely NO_x emissions of gas boilers (in steady state) were measured between 3 and 7 ppm, which is rather low. Using Equation (3) and thus considering the O_2 percentage measurement (not shown in Table 10), those figures can be converted in the 6.7-14.2 mg/kWh range, which is slightly better than provided by the literature (see combustion only figures reported in Table 3). The lower part of that range, i.e. 6.7 mg/kWh, corresponds to the gas boiler of the PEMFC hybrid system, and it is indeed under the 7.2 mg/kWh figure announced by the manufacturer. For the other classical gas condensing boiler, it is also under the announced value of 20 mg/kWh (as seen in the *Tested systems* section). In comparison, the diesel Euro 6 engine showed NO_x concentrations of 55 ppm in neutral and 40 ppm at 1500 rpm (without any load since the clutch was not engaged). Equation (3) and the coefficients of Table 9 being only relevant for natural gas appliances, another conversion equation from ppm to mg/kWh provided by literature for diesel engines has been implemented (Pilusa et al., 2012). Considering a molar mass of NO of 30, these NO_x emission concentrations correspond to the 173-238 mg/kWh range, i.e. under but close to the maximum NO_x Real Driving Emissions announced at about 280 mg/kWh, assuming an average consumption of 6L per 100 km (as seen in the *Tested systems* section). It also approximately corresponds to the emissions of an old oil-fired boiler (as seen in Table 3).

For all tested systems except the gas absorption heat pump, the NO_2 emissions are either nil or quite low compared to NO emissions, which was expected as NO has been reported to be the predominant nitrogen oxide emitted by combustion devices (Bowman, 1975).

For the gas absorption heat pump, NO_2 and NO emission levels are similar. The total NO_x emission level was measured at 42.3 mg/kWh. Those values are about three times greater than the tested classical gas condensing boiler given the worse NO_x results. Although the system is reported to belong to the NO_x class 5 (Robur, 2020), the system still exhibits NO_x emissions levels below the limit of class 6, i.e. the most stringent emission class reported in Table 6 according to the applicable standards.

There were no CO emissions regarding the steady state operating conditions of the PEMFC system (other than an explicable peak that is similar to the transient CO peak that occurs at the PEMFC startup, as seen in Figure 6). This was expected since CO is a major pollutant of PEMFC stacks and since it has been reported that the system is equipped with a CO-removing apparatus in the fuel (natural gas) processing system before the stack (Paulus et al., 2024). Transient CO peaks are surely not caused by the fuel cell stack but by the fuel processor of the PEMFC system. For example, it could happen when the reforming processes start and are not yet at their steady state temperature levels, impeding the CO remover from operating efficiently. During these transients for which CO can occur, the PEMFC stack must indeed surely be bypassed (Paulus et al., 2024). Also, because methane reforming requires temperatures much higher than the one occurring in the PEMFC stack, it has been reported that the PEMFC system involves an afterburner for reforming purposes (Paulus et al., 2024). In addition to burning the stack exhaust gases when the PEMFC is running (the anode exhaust still contains unused hydrogen and the cathode contains an excess of air, which is at a higher temperature than the ambient air), this afterburner also requires a direct feed from the natural gas supply to ensure enough heat for the reforming processes (Paulus et al., 2024). The inexplicable CO peak while the PEMFC was running is likely to be related to this afterburner (after the stack) and it can once again be assumed that no CO has gone through the PEMFC stack.

Oppositely, the SOFC system (two different machines of the same reference tested) showed slight CO emissions (5 ppm, 11 ppm, and 8 ppm respectively at 500 W_{el}, 1000 W_{el}, and 1500 W_{el} of power output) with no dependence on the thermal output or on the exhaust gases temperature (driven by the return temperature of the heat recovery system). Through Equation (3), these CO concentrations respectively correspond to 28.3 mg/kWh, 41.5 mg/kWh, and 17.0 mg/kWh. It is worth mentioning that the PEMFC system was mainly tested in field-test real applications so the return temperature (and the exhaust gas temperature) could not be controlled, although it is not believed to affect the pollutant emissions in steady state (which were nil).

CO emissions peak (between 50 and 60 ppm) at gas condensing boilers startup is probably due to the momentary incomplete combustion in this highly transient starting process. In steady state, the tested machines showed 8 to

30 ppm of CO emissions, corresponding to 10.7 mg/kWh to 40.7 mg/kWh using Equation (3), i.e. very similar to the CO emissions range of the SOFC). The gas condensing boilers were tested in field-test applications so the return temperature (and therefore the exhaust gases temperature) could not be controlled. Regarding the diesel engine, the steady state CO emissions were much higher, between 200 and 300 ppm at idle and up to 850 ppm at 1500 rpm. Equation (3) and the coefficients of Table 9 can only be used with natural gas. Therefore, another conversion law has been found in the literature (Pilusa et al., 2012), which leads to the 800-1200 mg/kWh range at idle and to about 3430 mg/kWh for the 1500 rpm test. Those levels of CO emissions are far greater than the one announced on the certificate of conformity for the average NEDC (calculated in this work to about 145 mg/kWh, as seen in the *Tested systems* section). This is another proof of the inadequacy of the NEDC to account for pollutant emissions (Pavlovic et al., 2017) but it also should be reminded that maintaining the engine at 1500 rpm while keeping the vehicle stationary is also not exactly representative of real driving conditions (although it provides interesting results for comparisons).

CO emissions of the tested gas absorption heat pump (120 ppm, corresponding to 153.7 mg/kWh related to the fuel input) are about four times greater than the tested gas condensing boilers giving the worse CO emissions results.

Regarding NO_x, SO_2, and CO emissions of residential fuel cells, the results of this research are in fact aligned with the insufficiently documented and unverified previous papers (as detailed in the *Pollutant emissions of residential fuel cells* section).

As implied in the *Measurements device* section and especially since its pollutant levels have been measured especially low, the laboratory tests conducted on the fuel cells could also have been performed with fixed continuous NO_x/SO_2 analysers for optimal resolution and accuracy. For example, the NO_x analyser '4000VML' (Signal Instruments, 2006) and/or the SO_2 analyser 'Serinus 50' (acoem, 2023) could have been used, at least if the actual SO_2 emission levels are not completely nil as opposed to what this study tends to indicate (in which case, investing in an additional SO_2 sensor would have been quite pointless). However, more accurate fixed sensors would not have changed the statements inferred by this study regarding the low pollutant levels exhibited by the fuel cells. In addition, for all the tests conducted in field-test applications, it was mandatory to use a portable sensor (such as the one used in this study).

The main limitation of this research comes from the fact that Volatile Organic Compounds (VOCs) but mostly Particulate Matter (PM) emissions were not considered in this study for the tested systems. Actually, an infructuous attempt to measure fine particulates has been made using the 'AFRISO STM 225' dust sensor (AFRISO-EURO-INDEX Group, 2018) in the exhaust chimney of the studied fuel cell systems. Indeed, as it can be seen in Figure 8 for the tested SOFC system, it is not possible to distinguish in the resulting signal any particulate matter emissions when the probe is placed in the exhaust chimney. This can mean three very different things: the fuel cells did not emit any fine particulates; the PM emissions could have been beneath the sensitivity range of the sensor, or the sensor might not have been optimally suited for natural gas flue gas analysis. This latter assumption is the most probable as the sensor is originally designed to measure dust concentration from pellets or wood-fired systems (AFRISO-EURO-INDEX Group, 2018). Unfortunately, no other PM sensor was available for this study at the time.

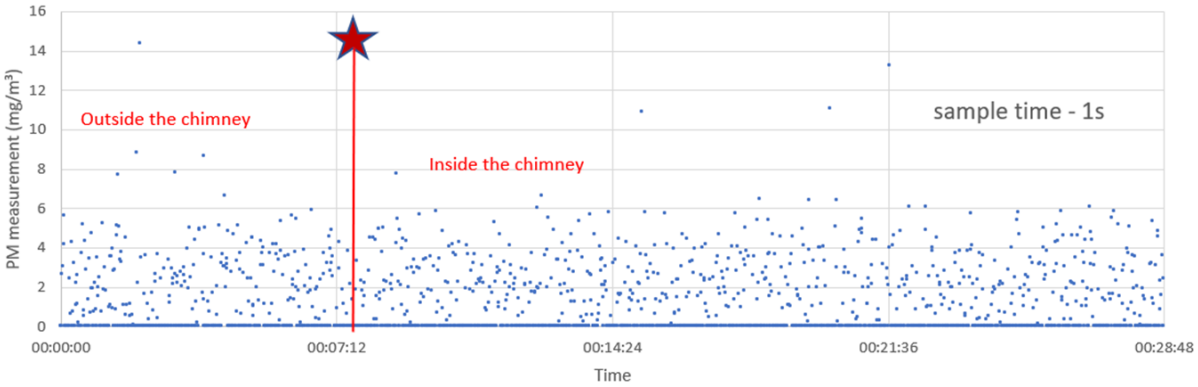

Figure 8. Example of signal from the fine particulates sensor 'AFRISO STM 225' for the studied SOFC system. There is absolutely no change in the signal when the probe is placed in ambient (external) air and when it is placed inside the fuel cell exhaust chimney.

Another limitation of this work lies in the validity of the comparison of emissions intensity per unit of energy (in g/kWh) between the Euro 6 vehicle and the tested space heating (or CHP) appliances. Indeed, in the Euro 6 standard (for heavy-duty vehicles), the pollutant intensity limits are defined in g/kWh based on the energy available in the engine (Martyr and Rogers, 2021). The conversion law used in this study for the tested light-duty vehicle uses the same definition of pollutant intensity (Pilusa et al., 2012), i.e. based on the engine's mechanical

energy. Therefore, it is not comparable as-is to the pollutant intensity (per unit of energy) also in g/kWh reported or measured for space heating appliances, i.e. referring to its low heating value fuel energy input (Fumey et al., 2018). This limitation is also applicable to the gas absorption heat pump. Indeed, its pollutant emissions measurements are related to the fuel input and not the heat generated at its output. Although it is commonly accepted that a classical gas condensing boiler has an average low heating value efficiency of 90% (Baldi et al., 2017; CWaPE, 2005), the tested gas absorption heat pump is announced by the manufacturer to achieve 169% of low heating value efficiency in some specific conditions (Robur, 2020). Therefore, even if it has been demonstrated that such gas absorption heat pumps are not likely to be that efficient in field-test applications (Dávila et al., 2022b), the pollutant emission levels should always be considered taking into account the thermal efficiency of the systems.

Similarly, when considering the pollutant intensity (per unit of energy) of the fuel cells tested in this study, it is crucial to recognize that these units function as cogeneration systems. They provide both electrical and thermal energy and yet, the pollutant measurement reported in g/kWh is only anchored to their fuel input. This distinct basis for measuring emissions intensity necessitates careful consideration when making direct comparisons across these different categories of energy-producing appliances (and vehicles).

Yet, another way of comparison could be thought of to provide perspectives about the impact of the different appliances. The proposed approach is based on the computation of their average total pollutant emissions yearly use. For example, considering an average Belgian household with 17500 kWh_{th} of space heating thermal demand per year (CREG, 2022) equipped with a classical gas condensing boiler of 90% of low heating value efficiency (Baldi et al., 2017; CWaPE, 2005), the related NO_x emissions of the space heating would correspond to the ones of only between 775 and 2660 km driven with the 6L/100km Euro 6 car (depending on the different results obtained for the tested gas condensing boilers). In other words, with that Euro 6 car, a 16000 km distance traveled over a year, as it is a common assumption in recent studies in developed countries (Amatuni et al., 2020), corresponds in terms of NO_x emissions to between 6 and 20 Belgian average households that use gas condensing boilers as space heating appliance.

Considering the tested gas absorption heat pump with an assumed (theoretical) seasonal efficiency of 150% (Dehghan B. et al., 2020) and again the average Belgian household with 17500 kWh_{th} of space heating thermal demand per year (CREG, 2022), the associated NO_x emissions levels would correspond to the ones about 4750 km driven with the 6L/100km Euro 6 car. The chosen example of an annual distance of 16000 km traveled by the tested car would thus correspond to a little more than three Belgian average households that use a gas absorption heat pump as their space heating appliance.

Similarly, based on its datasheet efficiencies, the yearly heat generation of the tested SOFC at its nominal power (1500 W_{el}) all year long can be estimated to about 5250 kWh_{th}, which would correspond to about 372 gCO produced over the year (based on the results of this study given in Table 10). Considering the CO emissions intensity respectively at idle and at 1500 rpm in neutral given in Table 10, this corresponds to only 180 to 775 km driven with the Euro 6 car. In other words, between 20 and 89 machines of the tested SOFC would be needed to match the CO emissions that account for an annual average driving distance of 16000 km (Amatuni et al., 2020) with the considered Euro 6 vehicle.

Although NO_x, SO_2, and CO levels of residential fuel cells have been demonstrated in this study to be very low, their market penetration also (and mainly) lies in their profitability and in the CO_2 savings they are allowing. Fortunately, the exact PEMFC and SOFC systems presented in this work have already been investigated in field-test applications regarding these matters in previous studies (Paulus et al., 2022a; Paulus and Lemort, 2022a). Two machines of each technology have been monitored in field-test applications for the whole year 2021. Their results have been summarized in Table 11 and Table 12. Those cost and CO_2 indicators are based on a comparison with (current) reference energy production systems with their own emission factors and costs. Those reference systems consist of electricity from the (Belgian) grid and heat from a gas-condensing boiler of 90% of LHV efficiency. The considered electrical price is 0.333€/kWh_{el} whereas the considered gas price is 0.093€/kWh_{HHV}, and they were approximately valid for residential bills in Belgium (and close to the Germany-France-Nederland average) in 2021 (CREG, 2024). Interestingly, according to the Belgian energy regulator, those energy costs are quite close to the 2023 ones in the same countries/regions (CREG, 2024). The gas consumption emission factor considered was 254 gCO_{2eq}/kWh_{LHV} and the Belgian grid consumption emission factor considered was the one computed hourly and provided by Electricity Maps (https://www.electricitymaps.com). For information, the statistical average of the Belgian grid electricity consumption emission factors in 2021 was 167 gCO_{2eq}/kWh_{el}.

It is noteworthy that the results reported in Table 11 and Table 12 are extremely case dependent and not only of energy costs. They are indeed dependent on the dwelling (and notably on its hydraulic installation), the way the system has been installed, the way the owner is using it, the owner's ability to consume the electrical production from the system, *etc*. Those indicators shall thus be considered with caution before being replicated in similar fuel

cell systems. Regarding costs and CO_2 balances, positive figures in Table 11 and Table 12 correspond to savings, so negative values indicate poorer performances than the reference systems.

Table 11.

2021 field-test cost and CO_2 indicators for two of the PEMFC-gas boiler hybrid system studied in this work. That year accounted for 2286 degree-days (Gas.be, 2021) according to the base 16.5°C (The Chartered Institution of Building Services Engineers, 2006)). Reproduced and adapted from reference (Paulus et al., 2022a).

Monitored data	PEMFC #1	PEMFC #2	Monitored data	PEMFC #1	PEMFC #2
HHV equivalent energy consumed (kWh)	20083	38243	LHV Electrical efficiency (%)	11.1	9.3
Electrical production (kWh)	2011	3222	LHV Thermal efficiency (%)	69.4	84.5
Electrical consumption (kWh)	298	258	LHV Total efficiency (%)	80.5	93.8
DHW (kWh)	1627	2095	Space heating (kWh)	10941	27061
Utilization cost savings (€)	≈1430	≈1300	Utilization CO_{2eq} savings ($kgCO_{2eq}$)	-469	-45

Table 12.

2021 field-test cost and CO_2 indicators for two of the SOFC system studied in this work. Climate hardiness is the same as reported in Table 11 but it is not as relevant as those SOFC systems are electrically driven and do not provide space heating (at least in the studied field-test sites). Reproduced and adapted from reference (Paulus and Lemort, 2022a).

Monitored data	SOFC #1	SOFC #2	Monitored data	SOFC #1	SOFC #2
HHV equivalent energy consumed (kWh)	25031	24273	LHV Electrical efficiency (%)	52.4	59.0
Electrical production (kWh)	11843	12922	LHV Thermal efficiency (%)	15.8	11.6
Electrical consumption (kWh)	11	2	LHV Total efficiency (%)	68.2	70.6
Heat recovered (kWh)	3569	2549	Utilization CO_{2eq} savings ($kgCO_{2eq}$)	-3013	-2969
Utilization cost savings (€)	≈-45	≈450			

From a global warming perspective, those systems are using fossil natural gas and Table 11 and Table 12 show that they cannot compete with the electrical grid (that involves renewables and should even involve more of those in the future). It must however be considered that in Belgium, in 2020 and 2021 (the author of this paper has not the information for 2022 and 2023), there was always some electrical production that came from natural gas power plants. Therefore, through the System Marginal Price (SMP) principle (Chae et al., 2012), the Marginal Emission Factor (MEF), which 'reflects the emissions intensities of the marginal generators in the system, i.e. the last generators needed to meet demand at a given time' (Siler-Evans et al., 2012), can always be considered equal to the emission factor for the electricity production from natural gas power plants. This would change the grid electricity emission factor to about three times more, i.e. to 456 gCO_{2eq}/kWh_{el} (Paulus et al., 2022a) and this would reverse the CO_2 balance of the SOFC systems to 700-1100 $kgCO_{2eq}$ savings (Paulus and Lemort, 2022a). This analysis is strengthened by the fact that SOFC systems are flexible in terms of electrical power output (within the 33-100% range for the system presented in this work) and could be controlled remotely to replace electrical production from natural gas power plants. In addition, the demonstrated electrical efficiencies of the studied SOFCs (Table 12) lie in the order of magnitude (and it is even slightly better for the SOFC #2) than typical natural gas power plants (Paulus and Lemort, 2022a). It is worth mentioning that decentralized local electrical production also avoids transportation and distribution losses, which can reach about 6-7% in the EU (Psomopoulos et al., 2010). This could have been considered in these ecological balances and they would actually be slightly improved.

The studied PEMFC system being not flexible in terms of power output and presenting at best a LHV electrical efficiency of 37% (Table 5), this Marginal Emission Factor approach is not as relevant and considered not applicable. Even so, it has been demonstrated in the mentioned previous study that the CO_2 balance of the studied PEMFC-gas boiler system could even remain negative (with the MEF assumption), at least for the PEMFC #1 (Paulus et al., 2022a).

Regarding energy utilization costs, the analyses are similar as the PEMFC-gas boilers systems can exhibit losses compared to reference systems (as indicated for the PEMFC #1 in Table 11) and as the SOFCs indicate significant yearly savings (Table 12). For instance, with the results of Table 12, if an investor wanted to ensure reaching a return on investment before 10 years, the maximum capital costs of the system (including installation) should not reach more than about 13-14 k€, considering that the owner already has a main space heating appliance (Paulus and Lemort, 2022a). Although this SOFC's capital costs are unknown to the authors, it is interesting to point out

that back in 2015, residential SOFC technology cost (with auxiliaries) was estimated at the time to be about 10 k€/kW (Napoli et al., 2015), i.e. quite close to that cost threshold.

These are the probable reasons why it has been reported that historical PEMFC manufacturers concluded that the future of fuel cells in domestic built environment applications lies with SOFCs, and have therefore stopped PEMFC development (Elmer et al., 2015).

6. Conclusion

The SO_2 and NO_x emission factors of (Belgian) grid electricity and common space heating appliances reproduced in this work represent an interesting contribution of this paper. In addition, this study has documented and reported equations that allow for converting pollutant concentration measurements, i.e. in ppm, into pollutant intensity per unit of energy, i.e. in mg/kWh, useful for comparative benchmarking analysis (especially considering the SO_2 and NO_x emissions factors reported in this paper).

As a final conclusion, both tested residential fuel cell technologies fed by natural gas can be considered clean regarding SO_2 and NO_x emissions. In addition, the CO emissions can be considered quite low for the tested SOFC and even nil for the tested PEMFC. Those statements apply even with machines that have already been running for up to 45000 hours. Therefore, the biggest issue of natural gas fuel cell technologies still lies in the CO_2 emissions associated with the fossil fuel they consume.

However, this study still demonstrated that the gas condensing boiler embodied within the tested PEMFC-gas boiler hybrid system exhibited many undesired ON/OFF cycling (with associated small NO_x and CO peaks). It is strongly believed that the high level of hybridization between the fuel cell and the gas boiler (seen in Figure 2) is responsible for those many unexpected boiler startups and shutdowns and therefore prevents both sub-systems from operating as optimally and reliably as they would have as standalone units.

At last, this research established that the tested gas absorption heat pump gives worse NO_x and CO emission levels than classical gas condensing boilers, even when considering that the gas absorption heat pump may exhibit an increased thermal efficiency of about 150% on a low heating value basis (Dehghan B. et al., 2020).

Funding

This work was conducted with the partial financial support of Gas.be without any involvement in study design; in the collection, analysis, and interpretation of data; in the writing of the report; and in the decision to submit the article for publication. It is noteworthy that the Gas.be company also provided the pollutant testing sensors.

CRediT authorship contribution statement

Nicolas Paulus: Conceptualization, Formal analysis, Investigation, Resources, Data curation, Methodology, Software, Writing – original draft, Writing – review & editing, Visualization. **Vincent Lemort:** Funding acquisition, Writing – review & editing, Supervision, Project administration, Validation.

Declaration of competing interest

The authors declare that they have no known competing financial interests or personal relationships that could have appeared to influence the work reported in this paper.

Data availability

Data will be made available on request.

Acknowledgements

The authors would thus like to thank the Gas.be company for its funding and hardware contributions. The authors would also like to thank Camila Dávila for conducting the pollutant tests on the gas absorption heat pump as well as providing the corresponding experimental data. At last, the main author would like to extend sincere gratitude to Valéry Broun, Director of the Industrial Engineering Higher Education Institution of the Province of Liège (HEPL), for accommodating the class schedules to allow room for such research activities.

References

acoem, 2023. Serinus® 50 - Sulfur Dioxide Analyser. Doc N°20230220.

acoem, 2022. Serinus® 40 - Oxides of Nitrogen Analyser. Doc N°20221214.

AFRISO-EURO-INDEX Group, 2019. MULTILYZER® STx - Analyseur de service. FR19001.

AFRISO-EURO-INDEX Group, 2018. Systronik - STM 225 Dust monitor. FR 18001.

Aguiar, P., Chadwick, D., Kershenbaum, L., 2004. Effect of methane slippage on an indirect internal reforming solid oxide fuel cell. Chem Eng Sci 59, 87–97. https://doi.org/10.1016/j.ces.2003.09.022

Alshorman, A.A., 2016. Characteristic Study of Bio-Membrane PEM Fuel Cell for Performance Upgrading. Procedia Comput Sci 83, 839–846. https://doi.org/10.1016/j.procs.2016.04.174

Amatuni, L., Ottelin, J., Steubing, B., Mogollón, J.M., 2020. Does car sharing reduce greenhouse gas emissions? Assessing the modal shift and lifetime shift rebound effects from a life cycle perspective. J Clean Prod 266, 121869. https://doi.org/10.1016/j.jclepro.2020.121869

Asiaban, S., Kayedpour, N., Samani, A.E., Bozalakov, D., De Kooning, J.D.M., Crevecoeur, G., Vandevelde, L., 2021. Wind and Solar Intermittency and the Associated Integration Challenges: A Comprehensive Review Including the Status in the Belgian Power System. Energies (Basel) 14. https://doi.org/10.3390/EN14092630

AVL, 2021. AVL DIGAS 444N. Spectrum + 919811031725.

Balamurugan, T., Nalini, R., 2014. Experimental investigation on performance, combustion and emission characteristics of four stroke diesel engine using diesel blended with alcohol as fuel. Energy 78, 356–363. https://doi.org/10.1016/j.energy.2014.10.020

Bălănescu, D.T., Homutescu, V.M., 2018. Experimental investigation on performance of a condensing boiler and economic evaluation in real operating conditions. Appl Therm Eng 143, 48–58. https://doi.org/10.1016/j.applthermaleng.2018.07.082

Bălănescu, D.-T., Homutescu, V.-M., 2017. Experimental Study on the Combustion System Optimization in the Case of a 36 kW Condensing Boiler. Procedia Eng 181, 706–711. https://doi.org/10.1016/j.proeng.2017.02.453

Baldi, F., Moret, S., Tammi, K., Maréchal, F., 2020. The role of solid oxide fuel cells in future ship energy systems. Energy 194, 116811. https://doi.org/10.1016/j.energy.2019.116811

Baldi, S., Quang, T. Le, Holub, O., Endel, P., 2017. Real-time monitoring energy efficiency and performance degradation of condensing boilers. Energy Convers Manag 136, 329–339. https://doi.org/10.1016/j.enconman.2017.01.016

Bang, E.-S., Kim, M.-H., Park, S.-K., 2022. Options for Methane Fuel Processing in PEMFC System with Potential Maritime Applications. Energies (Basel) 15, 8604. https://doi.org/10.3390/en15228604

Belgian Waste-To-Energy, n.d. Foire aux questions - FAQ [WWW Document]. URL http://www.bw2e.be/fr/foire-aux-questions-faq/ (accessed 4.18.23).

Bennett, G., Elwell, C., 2020. Effect of boiler oversizing on efficiency: a dynamic simulation study. Building Services Engineering Research & Technology 41, 709. https://doi.org/10.1177/0143624420927352

Bloom Energy, 2023. The Bloom Energy Server 5.5 [WWW Document]. Data Sheet. URL https://www.bloomenergy.com/wp-content/uploads/bloom-energy-server-datasheet-2023.pdf (accessed 5.29.23).

Bowman, C.T., 1975. Kinetics of pollutant formation and destruction in combustion. Prog Energy Combust Sci 1, 33–45. https://doi.org/10.1016/0360-1285(75)90005-2

Brook, R.D., Rajagopalan, S., Pope, C.A., Brook, J.R., Bhatnagar, A., Diez-Roux, A. V., Holguin, F., Hong, Y., Luepker, R. V., Mittleman, M.A., Peters, A., Siscovick, D., Smith, S.C., Whitsel, L., Kaufman, J.D., 2010. Particulate Matter Air Pollution and Cardiovascular Disease. Circulation 121, 2331–2378. https://doi.org/10.1161/CIR.0b013e3181dbece1

Bruijstens, A.J., Beuman, W.P.H., Molen, M.V.D., Rijke, J.D., Cloudt, R.P.M., Kadijk, G., Camp, O.O.D., Bleuanus, S., 2008. Biogas Composition and Engine Performance, Including Database and Biogas Property Model. BiogasMax.

Buderus, 2011. Installation instructions - Condensing gas boiler - Logamax plus GB142-24/30/45/60. 7215 0200 (11/2011) US/CA.

Cao, Y.-L., Yu, M.-X., Jiang, J., Cao, N.-N., Zhao, M., Wang, C., Zhang, D.-Q., Yan, J.-H., 2021. Effects of simulated acid rain on soil N2O emission from typical forest in subtropical sou-thern China. J Appl Ecol 32. https://doi.org/10.13287/j.1001-9332.202104.007

Chae, Y., Kim, M., Yoo, S.H., 2012. Does natural gas fuel price cause system marginal price, vice-versa, or neither? A causality analysis. Energy 47, 199–204. https://doi.org/10.1016/J.ENERGY.2012.09.047

Chameides, W.L., Fehsenfeld, F., Rodgers, M.O., Cardelino, C., Martinez, J., Parrish, D., Lonneman, W., Lawson, D.R., Rasmussen, R.A., Zimmerman, P., Greenberg, J., Mlddleton, P., Wang, T.,

1992. Ozone precursor relationships in the ambient atmosphere. J Geophys Res 97, 6037. https://doi.org/10.1029/91JD03014

Chartrand, R., 2011. Intergovernmental Advanced Stationary PEM Fuel Cell System Demonstration Final Report. US Department of Energy. https://doi.org/10.2172/1038683

Chen, D., Christensen, T.H., 2010. Life-cycle assessment (EASEWASTE) of two municipal solid waste incineration technologies in China. Waste Management & Research 28, 508–519. https://doi.org/10.1177/0734242X10361761

Cheremisinoff, N.P., 2002. Introduction to Air Quality, in: Handbook of Air Pollution Prevention and Control. Elsevier, pp. 1–52. https://doi.org/10.1016/B978-075067499-7/50002-X

Cheremisinoff, P.N., Young, R.A., 1977. Air pollution control and design handbook. Part II. Marcel Dekker, New York.

CREG, 2024. Analyse semestrielle de l'évolution des prix de l'énergie – 2ème semestre 2023.

CREG, 2022. Analyse semestrielle de l'évolution des prix de l'énergie – 2ème semestre 2021.

CREG, 2018. (F)1736 - Study on the cost-effectiveness of natural gas (CNG or compressed natural gas) used as fuel in cars. Commission de Régulation de l'Electricité et du Gaz.

CWaPE, 2005. Décision CD-5j18-CWaPE relative à "la définition des rendements annuels d'exploitation des installations modernes de référence, ..."

D2SERVICE, 2019. WP4: Design changes required for an easier and more competitive service of SP's μCHP appliance - D4.4: Service manual (prescriptions and instructions to installer). https://doi.org/10.3030/671473

Dávila, C., Paulus, N., Lemort, V., 2022a. Experimental investigation of a Micro-CHP unit driven by natural gas for residential buildings. Proceedings of the 19th International Refrigeration and Air Conditioning Conference (Herrick 2022).

Dávila, C., Paulus, N., Lemort, V., 2022b. Experimental Investigation of a Gas Driven Absorption Heat Pump and In-Situ Monitoring. Proceedings of the 9th Heat Powered Cycles International Conference (HPC 2021).

de Bruijn, F., 2005. The current status of fuel cell technology for mobile and stationary applications. Green Chemistry 7, 132. https://doi.org/10.1039/b415317k

de Gouw, J.A., Parrish, D.D., Frost, G.J., Trainer, M., 2014. Reduced emissions of CO2, NOx, and SO2 from U.S. power plants owing to switch from coal to natural gas with combined cycle technology. Earths Future 2, 75–82. https://doi.org/10.1002/2013EF000196

Dehghan B., B., Toppi, T., Aprile, M., Motta, M., 2020. Seasonal performance assessment of three alternative gas-driven absorption heat pump cycles. Journal of Building Engineering 31, 101434. https://doi.org/10.1016/j.jobe.2020.101434

Edelblute, C.M., Heller, L.C., Malik, M.A., Heller, R., 2015. Activated air produced by shielded sliding discharge plasma mediates plasmid DNA delivery to mammalian cells. Biotechnol Bioeng 112, 2583–2590. https://doi.org/10.1002/bit.25660

Eichhorn, L., Thudium, M., Jüttner, B., 2018. The Diagnosis and Treatment of Carbon Monoxide Poisoning. Dtsch Arztebl Int. https://doi.org/10.3238/arztebl.2018.0863

Element Energy, 2021. D1.7 - Summary report on specifications for newest model deployment in PACE. PACE - Pathway to a Competitive European Fuel Cell micro-CHP Market.

ELIA, 2023. Belgium's 2022 electricity mix: the increase in renewable energy and availability of nuclear power plants kept exports high. Brussels.

Elmer, T., Worall, M., Wu, S., Riffat, S.B., 2015. Fuel cell technology for domestic built environment applications: State of-the-art review. Renewable and Sustainable Energy Reviews 42, 913–931. https://doi.org/10.1016/j.rser.2014.10.080

Energie+, 2007. Emissions de polluants liée à la consommation énergétique [WWW Document]. URL https://energieplus-lesite.be/theories/consommation-energetique/les-emissions-de-polluants-liee-a-la-consommation-energetique/ (accessed 4.17.23).

European Commission, 2021. EN 15502-1 - Gas-fired heating boilers - Part 1: General requirements and tests.

European Commission, 2014. EN 12309-1 - Gas-fired sorption appliances for heating and/or cooling with a net heat input not exceeding 70 kW - Part 1: Terms and definitions.

European Commission, 2009. EN 590:2009 - Automotive fuels - Diesel - Requirements and test methods.

Fouad, F.H., Peters, R.W., Sisiopiku, V.P., Sullivan, A.J., Ahluwalia, R.K., 2007. Global Assessment of Hydrogen Technologies – Task 5 Report Use of Fuel Cell Technology in Electric Power Generation. Golden, CO (United States). https://doi.org/10.2172/923761

Fritsche, U., Rausch, L., 2009. Life Cycle Analysis of GHG and Air Pollutant Emissions from Renewable and Conventional Electricity, Heating, and Transport Fuel Options in the EU until 2030 - ETC/ACC Technical Paper 2009/18. Bilthoven.

Fuentes, E., Arce, L., Salom, J., 2018. A review of domestic hot water consumption profiles for application in systems and buildings energy performance analysis. Renewable and Sustainable Energy Reviews 81, 1530–1547. https://doi.org/10.1016/J.RSER.2017.05.229

Fumey, B., Buetler, T., Vogt, U.F., 2018. Ultra-low NOx emissions from catalytic hydrogen combustion. Appl Energy 213, 334–342. https://doi.org/10.1016/j.apenergy.2018.01.042

Galloway, J.N., Leach, A.M., Bleeker, A., Erisman, J.W., 2013. A chronology of human understanding of the nitrogen cycle. Philosophical Transactions of the Royal Society B: Biological Sciences 368, 20130120. https://doi.org/10.1098/rstb.2013.0120

Gas.be, 2021. Historique des degrés-jours à partir de 1961 [WWW Document]. URL https://a.storyblok.com/f/174880/x/b6820dc58a/jaar-2021-total.xls (accessed 5.4.24).

Geddes, J.A., Murphy, J.G., 2012. The science of smog: a chemical understanding of ground level ozone and fine particulate matter, in: Metropolitan Sustainability. Elsevier, pp. 205–230. https://doi.org/10.1533/9780857096463.3.205

Graedel, T.E., 1976. Sulfur dioxide, sulfate aerosol, and urban ozone. Geophys Res Lett 3, 181–184. https://doi.org/10.1029/GL003i003p00181

Grzywa-Celińska, A., Krusiński, A., Milanowski, J., 2020. 'Smoging kills' – Effects of air pollution on human respiratory system. Annals of Agricultural and Environmental Medicine 27, 1–5. https://doi.org/10.26444/aaem/110477

Guney, M.S., Tepe, Y., 2017. Classification and assessment of energy storage systems. Renewable and Sustainable Energy Reviews 75, 1187–1197. https://doi.org/10.1016/j.rser.2016.11.102

Gupta, P., 2018. Environmental and ecotoxicology, in: Illustrated Toxicology. Elsevier, pp. 373–425. https://doi.org/10.1016/B978-0-12-813213-5.00014-6

Haeseldonckx, D., D'haeseleer, W., 2007. The use of the natural-gas pipeline infrastructure for hydrogen transport in a changing market structure. Int J Hydrogen Energy 32, 1381–1386. https://doi.org/10.1016/J.IJHYDENE.2006.10.018

Hall, J.E., Hooker, P., Jeffrey, K.E., 2021. Gas detection of hydrogen/natural gas blends in the gas industry. Int J Hydrogen Energy 46, 12555–12565. https://doi.org/10.1016/j.ijhydene.2020.08.200

Hamra, G.B., Guha, N., Cohen, A., Laden, F., Raaschou-Nielsen, O., Samet, J.M., Vineis, P., Forastiere, F., Saldiva, P., Yorifuji, T., Loomis, D., 2014. Outdoor Particulate Matter Exposure and Lung Cancer: A Systematic Review and Meta-Analysis. Environ Health Perspect 122, 906–911. https://doi.org/10.1289/ehp/1408092

Hanrahan, G., 2012. Air Pollutants and Associated Chemical and Photochemical Processes, in: Key Concepts in Environmental Chemistry. Elsevier, pp. 215–242. https://doi.org/10.1016/B978-0-12-374993-2.10007-X

Jedlikowski, A., Englart, S., Cepiński, W., Badura, M., Ara Sayegh, M., 2020. Reducing energy consumption for electrical gas preheating processes. Thermal Science and Engineering Progress 19, 100600. https://doi.org/10.1016/j.tsep.2020.100600

Jiang, L., Hiltunen, E., He, X., Zhu, L., 2016. A Questionnaire Case Study to Investigate Public Awareness of Smog Pollution in China's Rural Areas. Sustainability 8, 1111. https://doi.org/10.3390/su8111111

Johnson, C.E., Derwent, R.G., 1996. Relative radiative forcing consequences of global emissions of hydrocarbons, carbon monoxide and NOx from human activities estimated with a zonally-averaged two-dimensional model. Clim Change 34, 439–462. https://doi.org/10.1007/BF00139301

Karvountzi, G.C., Duby, P.F., 2008. Comparison of a Multi-Megawatt High Temperature Fuel Cell System With Reciprocating Engines and Aero-Derivative Gas Turbines, in: Volume 8: Energy

Systems: Analysis, Thermodynamics and Sustainability; Sustainable Products and Processes. ASMEDC, pp. 741–749. https://doi.org/10.1115/IMECE2008-68933

Kee, R.J., Zhu, H., Sukeshini, A.M., Jackson, G.S., 2008. Solid Oxide Fuel Cells: Operating Principles, Current Challenges, and the Role of Syngas. Combustion Science and Technology 180, 1207–1244. https://doi.org/10.1080/00102200801963458

Kistner, L., Schubert, F.L., Minke, C., Bensmann, A., Hanke-Rauschenbach, R., 2021. Techno-economic and Environmental Comparison of Internal Combustion Engines and Solid Oxide Fuel Cells for Ship Applications. J Power Sources 508, 230328. https://doi.org/10.1016/j.jpowsour.2021.230328

Krist, K., 1999. SOFC-Based Residential Cogeneration Systems. ECS Proceedings Volumes 1999–19, 107–115. https://doi.org/10.1149/199919.0107PV

Kuo, Y.-M., Zhao, E., Li, M.-J., Yu, H., Qin, J., 2017. Ambient Precursor Gaseous Pollutants and Meteorological Conditions Controlling Variations of Particulate Matter Concentrations. Clean (Weinh) 45, 1600655. https://doi.org/10.1002/clen.201600655

Lammel, G., Graßl, H., 1995. Greenhouse effect of NOX. Environmental Science and Pollution Research 2, 40–45. https://doi.org/10.1007/BF02987512

Landis, M.S., Edgerton, E.S., 2024. Field intercomparison of continuous ambient FRM and FEM NO2 instruments in the Athabasca Oil Sands Region, Alberta, Canada and the potential impact on ambient regulatory compliance. J Air Waste Manage Assoc 74, 11–24. https://doi.org/10.1080/10962247.2023.2279169

Lichtenegger, K., Hebenstreit, B., Pointner, C., Schmidl, C., Höftberger, E., 2015. The role of leak air in a double-wall chimney. Heat and Mass Transfer 51, 787–794. https://doi.org/10.1007/s00231-014-1454-6

Martyr, A.J., Rogers, D.R., 2021. Engine exhaust emissions, in: Engine Testing. Elsevier, pp. 599–651. https://doi.org/10.1016/B978-0-12-821226-4.00017-6

McDonald, R., 2009. Evaluation of Gas, Oil and Wood Pellet Fueled Residential Heating System Emissions Characteristics. Upton, NY (United States). https://doi.org/10.2172/1015127

Minei, Y., Okajima, K., Yasuda, M., Ube, R., 2020. PEMFC System for Utilization of Exhaust Gas from Bright Heat Treatment furnace. Proceedings of the 12th International Conference on Applied Energy (ICAE2020). https://doi.org/10.46855/energy-proceedings-7263

Mishra, S., 2017. Is smog innocuous? Air pollution and cardiovascular disease. Indian Heart J 69, 425–429. https://doi.org/10.1016/j.ihj.2017.07.016

Muret, J., Fernandes, T.D., Gerlach, H., Imberger, G., Jörnvall, H., Lawson, C., McGain, F., Mortimer, F., Pauchard, J.-C., Pierce, T., Shinde, S., Swinton, F., Williams, L., 2019. Environmental impacts of nitrous oxide: no laughing matter! Comment on Br J Anaesth 2019; 122: 587–604. Br J Anaesth 123, e481–e482. https://doi.org/10.1016/j.bja.2019.06.013

Napoli, R., Gandiglio, M., Lanzini, A., Santarelli, M., 2015. Techno-economic analysis of PEMFC and SOFC micro-CHP fuel cell systems for the residential sector. Energy Build 103, 131–146. https://doi.org/10.1016/j.enbuild.2015.06.052

Papadopoulo, M., Kaddouh, S., Pacitto, P., Prieur-Vernat, A., 2011. Life Cycle Assessment of the European Natural Gas Chain focused on three environmental impact indicators. Brussels.

Park, B., Kim, S., Park, S., Kim, M., Kim, T.Y., Park, H., 2021. Development of Multi-Item Air Quality Monitoring System Based on Real-Time Data. Applied Sciences 11, 9747. https://doi.org/10.3390/app11209747

Park, J.O., Hong, S.-G., 2016. Design and Optimization of HT-PEMFC MEAs, in: High Temperature Polymer Electrolyte Membrane Fuel Cells. Springer International Publishing, Cham, pp. 331–352. https://doi.org/10.1007/978-3-319-17082-4_16

Parravicini, M., Barro, C., Boulouchos, K., 2020. Compensation for the differences in LHV of diesel-OME blends by using injector nozzles with different number of holes: Emissions and combustion. Fuel 259, 116166. https://doi.org/10.1016/j.fuel.2019.116166

Patnaik, P.P., Acharya, S.K., Padhi, D., Mohanty, U.K., 2016. Experimental investigation on CI engine performance using steam injection and ferric chloride as catalyst. Engineering Science and Technology, an International Journal 19, 2073–2080. https://doi.org/10.1016/j.jestch.2016.07.006

Paulus, Nicolas, 2024a. Comprehensive assessment of fuel cell types: A novel fuel cell classification system. To Be Submitted. https://doi.org/10.2139/ssrn.4800979

Paulus, Nicolas, 2024b. Decarbonization potentials of fuel cell technologies in micro-cogeneration application. Progress in Energy Under Review.

Paulus, N., 2024. Developing individual carbon footprint reduction pathways from carbon budgets: Examples with Wallonia and France. Renewable and Sustainable Energy Reviews 198, 114428. https://doi.org/10.1016/j.rser.2024.114428

Paulus, N., 2023. Confronting Nationally Determined Contributions (NDCs) to IPPC's +2°C carbon budgets through the analyses of France and Wallonia climate policies. Journal of Ecological Engineering 24. https://doi.org/10.12911/22998993/162984

Paulus, N., Dávila, C., Lemort, V., 2022a. Field-test economic and ecological performance of Proton Exchange Membrane Fuel Cells (PEMFC) used in micro-combined heat and power residential applications (micro-CHP). Proceedings of the 35th International Conference On Efficiency, Cost, Optimization, Simulation and Environmental Impact of Energy Systems (ECOS2022). https://doi.org/10.11581/dtu.00000267

Paulus, N., Dávila, C., Lemort, V., 2022b. Correlation between field-test and laboratory results for a Proton Exchange Membrane Fuel Cell (PEMFC) used as a residential cogeneration system. Proceeding of the 30th "Congrès Annuel de la Société Française de Thermique" (SFT 2022). https://doi.org/10.25855/SFT2022-119

Paulus, N., Job, N., Lemort, V., 2024. Investigation of degradation mechanisms and corresponding recovery procedures of a field-tested residential cogeneration Polymer Electrolyte Membrane fuel cell. To be submitted.

Paulus, N., Lemort, V., 2023a. Pollutant testing (NOx, SO2 and CO) of commercialized micro-combined heat and power (mCHP) fuel cells. Proceedings of the 36th International Conference On Efficiency, Cost, Optimization, Simulation and Environmental Impact of Energy Systems (ECOS2023). https://doi.org/10.52202/069564-0104

Paulus, N., Lemort, V., 2023b. Field-test performance models of a residential micro-cogeneration system based on the hybridization of a proton exchange membrane fuel cell and a gas condensing boiler. Energy Convers Manag 295. https://doi.org/10.1016/j.enconman.2023.117634

Paulus, N., Lemort, V., 2023c. Experimental investigation of a Solid Oxide Fuel Cell (SOFC) used in residential cogeneration applications. Proceedings of the 36th International Conference On Efficiency, Cost, Optimization, Simulation and Environmental Impact of Energy Systems (ECOS2023). https://doi.org/10.52202/069564-0056

Paulus, N., Lemort, V., 2023d. Establishing the energy content of natural gas residential consumption : example with Belgian field-test applications. IOP Conf Ser Earth Environ Sci 1185, 012013. https://doi.org/10.1088/1755-1315/1185/1/012013

Paulus, N., Lemort, V., 2022a. Field-test performance of Solid Oxide Fuel Cells (SOFC) for residential cogeneration applications. Proceedings of the 7th International High Performance Buildings Conference at Purdue (Herrick 2022).

Paulus, N., Lemort, V., 2022b. Grid-impact factors of field-tested residential Proton Exchange Membrane Fuel Cell systems. Proceedings of the 14th REHVA HVAC World Congress (CLIMA2022). https://doi.org/10.34641/CLIMA.2022.176

Pavlovic, J., Tansini, A., Fontaras, G., Ciuffo, B., Garcia Otura, M., Trentadue, G., Suarez Bertoa, R., Millo, F., 2017. The Impact of WLTP on the Official Fuel Consumption and Electric Range of Plug-in Hybrid Electric Vehicles in Europe. https://doi.org/10.4271/2017-24-0133

Payne, R., Love, J., Kah, M., 2009. Generating Electricity at 60% Electrical Efficiency from 1 - 2 kWe SOFC Products. ECS Trans 25, 231–239. https://doi.org/10.1149/1.3205530

Peng, R.D., 2008. Coarse Particulate Matter Air Pollution and Hospital Admissions for Cardiovascular and Respiratory Diseases Among Medicare Patients. JAMA 299, 2172. https://doi.org/10.1001/jama.299.18.2172

Perna, A., Minutillo, M., 2020. Residential cogeneration and trigeneration with fuel cells, in: Current Trends and Future Developments on (Bio-) Membranes. Elsevier, pp. 197–239. https://doi.org/10.1016/B978-0-12-817807-2.00009-5

Pilusa, T.J., Mollagee, M.M., Muzenda, E., 2012. Reduction of Vehicle Exhaust Emissions from Diesel Engines Using the Whale Concept Filter. Aerosol Air Qual Res 12, 994–1006. https://doi.org/10.4209/aaqr.2012.04.0100

Portmann, R.W., Daniel, J.S., Ravishankara, A.R., 2012. Stratospheric ozone depletion due to nitrous oxide: influences of other gases. Philosophical Transactions of the Royal Society B: Biological Sciences 367, 1256–1264. https://doi.org/10.1098/rstb.2011.0377

Proszak-Miasik, D., Rabczak, S., 2018. Methods for reducing low emissions from heating devices in single- family housing. E3S Web of Conferences 45, 00069. https://doi.org/10.1051/E3SCONF/20184500069

Psomopoulos, C.S., Kaminaris, S.D., Ioannidis, G.Ch., Themelis, N.J., 2017. Contribution of WTE plants in EU's targets for renewables. A review until 2014. Proceedings of the 5th International Conference on Sustainable Solid Waste Management (ATHEN 2017).

Psomopoulos, C.S., Skoula, I., Karras, C., Chatzimpiros, A., Chionidis, M., 2010. Electricity savings and CO2 emissions reduction in buildings sector: How important the network losses are in the calculation? Energy 35, 485–490. https://doi.org/10.1016/j.energy.2009.10.016

Rabiu, A.M., Dlangamandla, N., Ulleberg, Ø., 2012. Novel Heat Integration in a Methane Reformer and High Temperature PEM Fuel Cell-based mCHP System. APCBEE Procedia 3, 17–22. https://doi.org/10.1016/j.apcbee.2012.06.039

Rana, M., Mittal, S.K., Beig, G., 2019. Enhanced Ozone Production in Ambient Air at Patiala Semi-Urban Site During Crop Residue Burning Events. MAPAN 34, 273–288. https://doi.org/10.1007/s12647-019-00315-x

Raza, W., Saeed, S., Saulat, H., Gul, H., Sarfraz, M., Sonne, C., Sohn, Z.-H., Brown, R.J.C., Kim, K.-H., 2021. A review on the deteriorating situation of smog and its preventive measures in Pakistan. J Clean Prod 279, 123676. https://doi.org/10.1016/j.jclepro.2020.123676

Robur, 2022. Abso | K18 Simplygas Heat Pump. ENG X-DPL306.

Robur, 2020. Handbook for the K18 range. D-MNL049 - Rev J.

Rotmans, J., Den Elzen, M.G.J., 1992. A model-based approach to the calculation of global warming potentials (GWP). International Journal of Climatology 12, 865–874. https://doi.org/10.1002/joc.3370120809

Rypdal, K., Rive, N., Berntsen, T., Fagerli, H., Klimont, Z., Mideksa, T.K., Fuglestvedt, J.S., 2009. Climate and air quality-driven scenarios of ozone and aerosol precursor abatement. Environ Sci Policy 12, 855–869. https://doi.org/10.1016/j.envsci.2009.08.002

Schumann, P., Graf, C., Friedrich, K.A., 2008. Modeling and Simulation of a PEM Fuel Cell System for Aircraft Applications. ECS Trans 12, 651–661. https://doi.org/10.1149/1.2921590

Sharaf, O.Z., Orhan, M.F., 2014. An overview of fuel cell technology: Fundamentals and applications. Renewable and Sustainable Energy Reviews 32, 810–853. https://doi.org/10.1016/J.RSER.2014.01.012

Sher, E., 1998. Environmental Aspects of Air Pollution, in: Handbook of Air Pollution From Internal Combustion Engines. Elsevier, pp. 27–41. https://doi.org/10.1016/B978-012639855-7/50041-7

Shipley, A.M., Elliott, R.N., 2004. Phantom Power: The Status of Fuel Cell Technology Markets. Energy Engineering 101, 26–45. https://doi.org/10.1080/01998590409509255

Signal Instruments, 2006. Model 4000VML Heated Vacuum Chemiluminescent NOx Analyser. 4000VML.pdf/2006.

Siler-Evans, K., Azevedo, I.L., Morgan, M.G., 2012. Marginal Emissions Factors for the U.S. Electricity System. Environ Sci Technol 46, 4742–4748. https://doi.org/10.1021/es300145v

Sillman, S., 2003. Tropospheric Ozone and Photochemical Smog, in: Treatise on Geochemistry. Elsevier, pp. 407–431. https://doi.org/10.1016/B0-08-043751-6/09053-8

Solomon, J.M., Pachamuthu, S., Arulanandan, J.J., Thangavel, N., Sathyamurthy, R., 2020. Electrochemical decomposition of NOx and oxidation of HC and CO emissions by developing electrochemical cells for diesel engine emission control. Environmental Science and Pollution Research 27, 32229–32238. https://doi.org/10.1007/s11356-019-07327-9

Speight, J.G., 2019. Energy security and the environment, in: Natural Gas: A Basic Handbook. Gulf Professional Publishing, pp. 361–390. https://doi.org/10.1016/B978-0-12-809570-6.00010-2

Srinivasan, S., Miller, E., 2006. Applications and economics of fuel-cell power plants/power sources, in: Fuel Cells. Springer US, Boston, MA, pp. 575–605. https://doi.org/10.1007/0-387-35402-6_10

Teledyne API, 2021a. The Model T200 Chemiluminescence NO/NO2/NOx Analyzer. SAL000046J.

Teledyne API, 2021b. The Model T500U CAPS NO2 Analyzer. SAL000078J.

The Chartered Institution of Building Services Engineers, 2006. Degree-days: theory and application (TM41: 2006) [WWW Document]. URL https://www.cibse.org/knowledge-research/knowledge-portal/technical-memorandum-41-degree-days-theory-and-application-2006-pdf (accessed 7.4.23).

Thermo Scientific, 2021. The Thermo Scientific ™ Model 42i NO-NO2-NOx. EPM_42i_DS_0921.

Thomson, A.J., Giannopoulos, G., Pretty, J., Baggs, E.M., Richardson, D.J., 2012. Biological sources and sinks of nitrous oxide and strategies to mitigate emissions. Philosophical Transactions of the Royal Society B: Biological Sciences 367, 1157–1168. https://doi.org/10.1098/rstb.2011.0415

TSI Incorporated, 2004. An Overview of Measurements, Methods and Calculations Used in Combustion Analysis.

Turconi, R., Boldrin, A., Astrup, T., 2013. Life cycle assessment (LCA) of electricity generation technologies: Overview, comparability and limitations. Renewable and Sustainable Energy Reviews 28, 555–565. https://doi.org/10.1016/J.RSER.2013.08.013

Urdampilleta, I., Uribe, F., Rockward, T., Brosha, E.L., Pivovar, B., Garzon, F.H., 2007. PEMFC Poisoning with H2S: Dependence on Operating Conditions. ECS Trans 11, 831–842. https://doi.org/10.1149/1.2780996

Varma, D.R., Mulay, S., Chemtob, S., 2015. Carbon Monoxide, in: Handbook of Toxicology of Chemical Warfare Agents. Elsevier, pp. 267–286. https://doi.org/10.1016/B978-0-12-800159-2.00021-X

Venfield, H., Brown, A., 2018. Domestic Boiler Emission Testing. Doc N°60566063_1.

VHK for the European Commission, 2019. Space and combination heaters - Ecodesign and Energy Labelling. Task 1 - Scope – Policies & Standards.

Vrekoussis, M., Pikridas, M., Rousogenous, C., Christodoulou, A., Desservettaz, M., Sciare, J., Richter, A., Bougoudis, I., Savvides, C., Papadopoulos, C., 2022. Local and regional air pollution characteristics in Cyprus: A long-term trace gases observations analysis. Science of The Total Environment 845, 157315. https://doi.org/10.1016/j.scitotenv.2022.157315

Wade, J., Farrauto, R.J., 2012. Controlling emissions of pollutants in urban areas, in: Metropolitan Sustainability. Elsevier, pp. 260–291. https://doi.org/10.1533/9780857096463.3.260

Wagner, A.L., Wagner, J.P., Krause, T.R., Carter, J.D., 2002. Autothermal Reforming Catalyst Development for Fuel Cell Applications. Journal of Engines.

Wen, T., 2002. Material research for planar SOFC stack. Solid State Ion 148, 513–519. https://doi.org/10.1016/S0167-2738(02)00098-X

Xu, S., Deng, Y., Webb, K., Wright, H., Dimick, P.S., Cremaschi, S., Eden, M.R., 2020. Sour Gas Sweetening Technologies for Distributed Resources – A Process Simulation Study. Computer Aided Chemical Engineering 48, 1483–1488. https://doi.org/10.1016/B978-0-12-823377-1.50248-2

Zhou, B., Cui, T., Li, D., 2015. Climate Monitoring and Formation Mechanism of Smog Pollution in China. Chinese Journal of Urban and Environmental Studies 03. https://doi.org/10.1142/S234574811550013X

Zlateva, P., Penkova, N., Krumov, K., 2020. Analysis of combustion efficiency at boilers operating on different fuels, in: 2020 7th International Conference on Energy Efficiency and Agricultural Engineering (EE&AE). IEEE, pp. 1–4. https://doi.org/10.1109/EEAE49144.2020.9278784